Received: 5 November 2019 | Accepted: 21 April 2020

DOI: 10.1111/mec.15458

ORIGINAL ARTICLE

MOLECULAR ECOLOGY WILEY

Phylogenomics unravels Quaternary vicariance and allopatric speciation patterns in temperate-montane plant species: A case study on the *Ranunculus auricomus* species complex

Salvatore Tomasello[1] | **Kevin Karbstein**[1,2] | **Ladislav Hodač**[1] | **Claudia Paetzold**[1] | **Elvira Hörandl**[1]

[1]Department of Systematics, Biodiversity and Evolution of Plants (with Herbarium), Albrecht-von-Haller Institute for Plant Sciences, University of Goettingen, Göttingen, Germany

[2]Georg-August University School of Science (GAUSS), University of Goettingen, Goettingen, Germany

Correspondence
Salvatore Tomasello, Department of Systematics, Biodiversity and Evolution of Plants (with Herbarium), Georg August University Göttingen, Untere Karspüle 2, 37073 Göttingen, Germany.
Email: salvatore.tomasello@uni-goettingen.de

Funding information
German Research Foundation, Grant/Award Number: Ho4395/10-1

Abstract

The time frame and geographical patterns of diversification processes in European temperate-montane herbs are still not well understood. We used the sexual species of the *Ranunculus auricomus* complex as a model system to understand how vicariance versus dispersal processes in the context of Pleistocene climatic fluctuations have triggered speciation in temperate-montane plant species. We used target enrichment sequence data from about 600 nuclear genes and coalescent-based species tree inference methods to resolve phylogenetic relationships among the sexual taxa of the complex. We estimated absolute divergence times and, using ancestral range reconstruction, we tested if speciation was enhanced by vicariance or by dispersal processes. Phylogenetic relationships among taxa were fully resolved with some incongruence in the position of the tetraploid *R. marsicus*. Speciation events took place in a very short time at the end of the Mid-Pleistocene Transition (830–580 thousand years ago [ka]). A second wave of intraspecific geographical differentiation occurred at the end of the Riss glaciation or during the Eemian interglacial between 200 and 100 ka. Ancestral range reconstruction suggests a widespread European ancestor of the *R. auricomus* complex. Vicariance has triggered allopatric speciation in temperate-montane plant species during the climatic deterioration that occurred during the last phase of the Mid-Pleistocene Transition. Vegetation restructuring from forest into tundra could have confined these forest species into isolated glacial macro- and microrefugia. During subsequent warming periods, range expansions of these species could have been hampered by apomictic derivatives and by other congeneric competitors in the same habitat.

KEYWORDS

ancestral range, geodispersal, Mid-Pleistocene Transition, *Ranunculus auricomus* complex, target enrichment, vicariance

1 | INTRODUCTION

Pleistocene climatic fluctuations have caused periodic range shifts (e.g., north–south) and/or range expansions and contractions in northern hemisphere plant species. The alternation of cold and warm periods has characterized the entire Quaternary (the last 1.8 million years). In Europe, cold periods have produced southward shifts in the distribution ranges of temperate species (in the so-called "Mediterranean refugia"; Brewer, Cheddadi, de Beaulieu, Reille, & Contributors, 2002; Taberlet, Fumagalli, Wust-Saucy, & Cosson, 1998) and/or the survival of these in few, isolated central European refugial areas (e.g., Magri et al., 2006; Naydenov, Senneville, Beaulieu, Tremblay, & Bousquet, 2007). On the other hand, warmer interglacials have favoured range expansion towards the north and the formation of contact zones among diverged populations of the same species (Hewitt, 1999; Magri, 2008). As a result, the survival of formerly coherent population groups in isolated refugia promoted allopatric speciation. Range expansions and the consequent formation of secondary contact zones resulted in hybridization, and eventually in the formation of new taxa through homoploid hybrid speciation or allopolyploidization (Abbott et al., 2013; Stebbins, 1984).

In the last three decades, many studies have elucidated upon the distribution and diversification in European high-alpine plant species (see Schönswetter, Stehlik, Holderegger, & Tribsch, 2005; Vargas, 2003). Although many studies have highlighted the importance of vicariance and postglacial recolonization for explaining phylogeographical patterns in alpine plant species (Comes & Kadereit, 1998; Kropf, Kadereit, & Comes, 2003; Taberlet et al., 1998; Widmer & Lexer, 2001), sometimes the situation is rather complicated and not easily explained by either vicariance or dispersal (Reisch, 2008; Sanz, Schönswetter, Vallés, Schneeweiss, & Vilartesana, 2014; Schönswetter & Tribsch, 2005; Tomasello & Oberprieler, 2017; Tribsch, Schönswetter, & Stuessy, 2002). Cold periods have not exclusively influenced the actual species distribution and intraspecific genetic patterns of alpine species, they have also actively promoted divergence and speciation, as documented in studies on animals (Knowles, 2001) and plants (Kadereit, Griebeler, & Comes, 2004). In the latter study, the authors observed that speciation processes in *Primula* sect. *Auricula* occurred principally during glacial periods in geographically isolated refugia.

Much less information is available on montane and/or subalpine plant species of the northern hemisphere. Research of forest plants has focused on the dominating tree species, such as beech, oaks and pine (e.g., Brewer et al., 2002; Magri, 2008; Naydenov et al., 2007). However, herbaceous plants inhabiting the understorey of cool and deciduous mountain forests of the temperate biome have rarely been investigated (Alsos, 2005; Després, Loriot, & Gaudeul, 2002). In cold periods of the Pleistocene, large parts of Central Europe were dominated by steppe vegetation, and deciduous forests were mostly restricted to southern and main refugia in the Balkan and Iberian peninsulas (Stuchlik & Wójcik, 2001). However, more distant local microrefugia outside the main southern glacial refugial areas should also be considered (Rull, 2009). For the boreomontane species *Polygonatum verticillatum*, putative glacial refugia might have existed in the foothills of heavily glaciated mountain ranges, such as the Alps and the Carpathians (Kramp, Huck, Niketić, Tomović, & Schmitt, 2008). In warmer periods, the ecoclimatic barriers for forests disappeared, leaving only the highest chains of the Alps and Carpathians as a geographical barrier. Hence, reforestation of the lower elevational zones around these mountain areas and in the lowlands has provided ample opportunities for herbaceous understorey plants to expand their range via geodispersal. In contrast to "jump" dispersal over a persisting barrier, geodispersal describes a more or less continuous range expansion after disappearance of a barrier, and would result in a single, widespread species (Ronquist & Sanmartín, 2011; Sanmartín, 2012). Geodispersal was found to be important for boreotropical forest plants (Couvreur et al., 2011), but little is known for temperate forest plants. Zhao, Wang, Ma, Liang, and He (2013), for example, found vicariance and allopatric speciation in a temperate deciduous forest plant in China.

The cosmopolitan genus *Ranunculus* L. with ~600 species originated and started diversifying in the early Miocene (Emadzade & Hörandl, 2011). Emadzade, Gehrke, Linder, and Hörandl (2011) have elucidated how both vicariance and long-distance dispersal have to be invoked to explain the present distribution patters of lowland and montane species in the genus. Intercontinental and transoceanic dispersal of forest species occurred mostly in the *Ranunculus polyanthemos* clade (Emadzade et al., 2011). Other clades comprising forest species, such as *R.* sect. *Auricomus*, have not yet been fully resolved. The Eurasian *Ranunculus auricomus* complex is nested as a monophyletic group within this large clade (*R.* sect. *Auricomus*) that comprises otherwise Asian, Arctic and North American species (Emadzade et al., 2015). Whereas apomictic polyploids of the *R. auricomus* complex are widespread and abundant in various temperate and boreal biomes, by contrast sexuals are montane and subalpine species of Mediterranean and temperate European mountains, inhabiting deciduous forest ecosystems or natural and anthropogenic meadows. Although these forests are widespread over temperate Europe, these taxa have restricted or disjunct distribution ranges, and usually occur at the foothills of the main European mountain ranges (Figure 1). Both vicariance or jump dispersal could have shaped this pattern. It is also unclear why speciation occurred despite the lowland areas being connected during interglacial periods and providing habitats for geodispersal.

The whole *R. auricomus* complex shows a pattern of geographical parthenogenesis: sexual progenitors have much smaller and more southern distribution areas than the numerous polyploid apomictic derivatives (Bierzychudek, 1985; Hörandl, 2006). Apomictic lineages can expand their range rapidly due to uniparental reproduction, both via long-distance dispersal and geodispersal (Baker, 1967; Cosendai, Wagner, Ladinig, Rosche, & Hörandl, 2013; Hörandl, 2006; Kirchheimer et al., 2018). However, why sexual progenitors of such complexes do not manage to expand their distribution areas and fail to fill their potential range remain poorly understood (see e.g., simulations in Kirchheimer et al., 2018). Hence, it is important to disentangle the biogeographical histories and speciation processes of

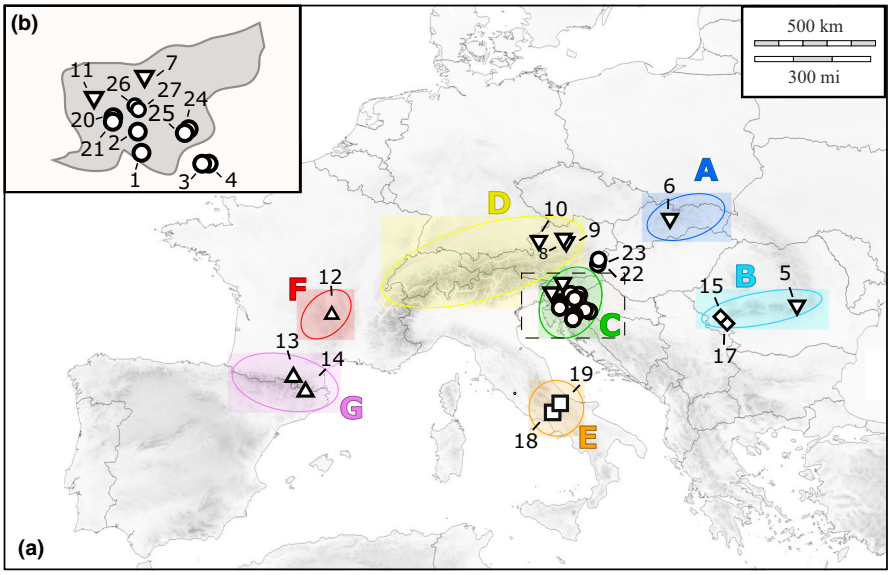

FIGURE 1 Distribution map of the accessions included in the present study (a) and detailed map of specimens collected in Slovenia (b). Numbers correspond to the map IDs in Table 1. Different symbols are for different species, following the treatment given in Karbstein et al. (2020): circles are for *Ranunculus notabilis* s.l., diamonds for *R. flabellifolius*, squares for *R. marsicus*, triangles for *R. envalirensis* s.l. and overturned triangles for *R. cassubicifolius* s.l. Coloured ellipses refer to the areas defined for the ancestral range reconstruction analysis: A, Northern Carpathians; B, Southern Carpathians; C, Illyrian region; D, Northern Prealps; E, Central Apennines; F, Massif Central; and G, Pyrenees

sexual species from their apomictic derivatives to understand the phenomenon of geographical parthenogenesis.

All taxa included herein are diploid or tetraploid sexuals (Dunkel, Gregor, & Paule, 2018; Hojsgaard et al., 2014; Masci, Miho, & Marchi, 1994). Hörandl (2004) estimated the divergence time between *R. notabilis* and *R. cassubicifolius* s.l. (including *R. carpaticola*) using isozyme data and Nei's genetic distances (Nei, 1975) as 914,000 years ago. Apomictic hybrid taxa are hypothesized to be even younger (<100,000 years; Pellino et al., 2013). Up to now, traditional markers have failed to resolve the phylogenetic relationships among taxa of the complex (Hörandl et al., 2009). Karbstein et al. (2020) applied phylogenomic methods (RADseq and target enrichment), together with geometric morphometrics to investigate species boundaries among the sexual taxa of the complex. The authors concluded that five species are recognizable within the complex (*R. cassubicifolius* s.l., *R. envalirensis* s.l., *R. flabellifolius*, *R. marsicus* and *R. notabilis* s.l.; Table 1).

In the present study, we address three major questions concerning the spatiotemporal diversification of temperate-montane species in Europe, using as study object the sexual species of the *R. auricomus* complex. (a) Did colder periods during glaciation cycles enhance speciation processes in temperate-montane species? (b) Is vicariance, dispersal or geodispersal the most probable scenario to explain the present distribution of sexual taxa of *R. auricomus*? (c) Did the species survive glacial periods in southern macrorefugia or also in microrefugia, and (if the latter scenario is the most plausible) why are they still restricted to these areas? Therefore, we: (a) applied target enrichment of nuclear genes to resolve phylogenetic relationships among taxa of the complex; (b) use coalescent-based methods to estimate the species divergence times in the context of past climatic oscillations; (c) apply ancestral range reconstruction methods to test vicariance versus dispersal speciation scenarios and identify potential macro- and microrefugia; and (d) discuss the relevance of our findings for understanding the geographical parthenogenesis pattern.

2 | MATERIALS AND METHODS

2.1 | Plant material

We included samples from all the described sexual species of the *Ranunculus auricomus* complex. Plant material used for DNA extraction consisted of silica-gel dried leaves or herbarium specimens (Table 1). We follow the taxonomy of Karbstein et al. (2020) (see synonymy in Table 1). Two additional *Ranunculus* species not belonging to the *R. auricomus* complex were included in the analyses as an outgroup: *R. pygmaeus* from the clade of *Ranunculus* sect. *Auricomus*, and *R. sceleratus* from the next sister clade (Emadzade et al., 2011).

2.2 | Gene selection and probe design

To find single-copy genes and select target regions for phylogenetic analyses, we used transcriptomes from two diploid species (*R. notabilis* and *R. cassubicifolius*, as synonym "*R. carpaticola*" in Pellino et al., 2013), a tetraploid sexual accession of *R. cassubicifolius* (Pellino et al., 2013), and *R. brotherusii* (Chen, Zhao, Wang, & Moody, 2015), an Asian species

TABLE 1 Information for the 28 accessions belonging to sexual taxa of the *Ranunculus auricomus* complex, and the two outgroup samples

ID	Map ID	Taxon	Locality	Collection date	Altitude	Latitude	Longitude	Range code	Herb. Voucher	Ploidy[a]
Du003-1[b]	1	"*R. austroslovenicus*" ***R. notabilis* s.l.**	Slovenia (SI)	23.04.2013	260	45.495278	14.803889	C	Du-30441	2*n*
LH012-8	2	"*R. austroslovenicus*" ***R. notabilis* s.l.**	Slovenia (SI)	03.05.2017	469	45.677445	14.82614	C		2*n*
2[b]	3	"*R. calapius*" ***R. notabilis* s.l.**	Croatia (HR)	10.04.2017	141	45.518944	15.570917	C	Du-34889	2*n*
Du-35351-15	4	"*R. calapius*" ***R. notabilis* s.l.**	Croatia (HR)	23.04.2018	117	45.51806	15.6125	C	Du-35351-15	2*n*
9126-2	5	"*R. carpaticola*" ***R. cassubicifolius* s.l.**	Romania (RO)	07.07.1998	1,360	45.432833	25.530708	AB		2*n*
Du013-1	6	"*R. carpaticola*" ***R. cassubicifolius* s.l.**	Hungary (HU)	19.04.2008	230	48.114122	20.653033	AB	Du-21047	2*n*
LH040-4	7	"*R. carpaticola*" ***R. cassubicifolius***	Slovakia (SK)	03.05.2018	387	48.67731	20.106684	AB		2*n*
LH008-7	8	***R. cassubicifolius***	Austria (AT)	01.05.2017	473	47.938828	14.94475	C		4*n*
LH009-3	9	***R. cassubicifolius***	Austria (AT)	01.05.2017	548	47.924792	14.972606	C		4*n*
LH006-17	10	***R. cassubicifolius***	Germany (DE)	30.04.2017	539	47.811203	12.506822	CD		2*n*
LH016-14	11	***R. cassubicifolius***	Slovenia (SI)	04.05.2017	514	46.010798	14.102718	CD		2*n*
Du-33354-2[b]	12	"*R. cebennensis*" ***R. envalirensis* s.l.**	France (FR)	06.05.2016	910	45.5605566	2.656944	F	Du-33354-2	2*n*
Du018-1[b]	13	***R. envalirensis***	Andorra (AD)	23.05.2013	1,750	42.591333	1.671583	G	Du-29983	2*n*
Du019[b]	14	***R. envalirensis***	France (FR)	23.05.2013	1,595	42.473278	2.080333	G	Du-29988	2*n*
Du021-1[b]	15	***R. flabellifolius***	Romania (RO)	21.04.2010	885	45.049444	21.771306	B	Du-25795	2*n*
Du054-1[b]	16	***R. flabellifolius***	Romania (RO)	21.04.2010	885	45.049444	21.771306	B	Du-25796	2*n*
LH025-1[b]	17	***R. flabellifolius***	Romania (RO)	10.04.2018	811	45.032008	21.78511	B		2*n*
LH017-1[b]	18	***R. marsicus***	Italy (IT)	26.06.2017	1,535	41.845403	13.929692	E		4*n*
LH018-2[b]	19	***R. marsicus***	Italy (IT)	27.06.2017	1,244	41.868211	14.021872	E		4*n*
LH014-3[b]	20	"*R. mediocompositus*" ***R. notabilis* s.l.**	Slovenia (SI)	03.05.2017	434	45.84954	14.25946	C		2*n*
LH015-10	21	"*R. mediocompositus*" ***R. notabilis* s.l.**	Slovenia (SI)	03.05.2017	436	45.848988	14.257088	C		2*n*
10137-3[b]	22	***R. notabilis***	Austria (AT)	08.05.2011	220	47.047778	16.4325	C		2*n*
Hoe5615	23	***R. notabilis***	Austria (AT)	05.05.1994	210	47.052739	16.38406	C	Hoe5615	2*n*
LH010-7[b]	24	"*R. peracris*" ***R. notabilis* s.l.**	Slovenia (SI)	02.05.2017	151	45.89075	15.370933	C		2*n*

(Continues)

TABLE 1 (Continued)

ID	Map ID	Taxon	Locality	Collection date	Altitude	Latitude	Longitude	Range code	Herb. Voucher	Ploidy[a]
LH011-1	25	"*R. peracris*" ***R. notabilis* s.l.**	Slovenia (SI)	02.05.2017	148	45.880803	15.336522	C		2*n*
LH011-14	25	"*R. peracris*" ***R. notabilis* s.l.**	Slovenia (SI)	02.05.2017	148	45.880803	15.336522	C		2*n*
Du049-1[b]	26	"*R. subcarniolicus*" ***R. notabilis* s.l.**	Slovenia (SI)	26.04.2016	325	45.944056	14.653083	C	Du-33266	2*n*
LH013-3[b]	27	"*R. subcarniolicus*" ***R. notabilis* s.l.**	Slovenia (SI)	03.05.2017	324	45.945453	14.651618	C		2*n*
Outgroups										
LG09		*R. pygmaeus*	Alaska (US)	07.11.2009	2	64.4561	−165.0961		LG09-A-47-07	2*n*
10426-3		*R. scleratus*	Germany (DE)	15.04.2018	165	51.5789	10.1458			2*n*

Note: Accepted names following Karbstein et al. (2020) are in bold type, and younger synonyms are in inverted commas. Countries are abbreviated according to ISO code 3166-2. Altitude is given in metre above sea level (m a.s.l.). Range codes are those used in BIOGEOBEARS for the ancestral range reconstruction and correspond to those in Figure 1. Map IDs refer to the samples IDs given in Figure 1.

[a]After Masci et al. (1994), Hojsgaard et al. (2014), Dunkel et al. (2018) and Karbstein et al. (2020).

[b]Samples from type material or collected from "locus classicus" and nearby.

of *R.* sect. *Auricomus*. MARKERMINER version 1.0 (Chamala et al., 2015) was used to identify putative single-copy orthologous loci for probe design with *Arabidopsis thaliana* as reference. We selected exons found in at least two of the four transcriptomes, with lengths ranging from 120 to 960 bp and a minimum variability of two single nucleotide polymorphisms (SNPs)/120 bp, using a custom python script (available at: https://github.com/ClaudiaPaetzold/MarkerMinerFilter.git). We identified 2,628 exonic regions belonging to 736 target genes (Table S1). The selected target regions (genes) ranged from 121 to 5,291 bp and included at least one exonic fragment each.

Arbor Biosciences produced a MYbaits Target Enrichment kit with 20,000, 120-bp-long, in-solution, biotinylated baits based on target sequence information. The final bait panel consisted of 17,988 probes, 14,632 of which are unique, and tiling at 2 × density.

2.3 | Library preparation

Sequencing libraries were prepared using either the "NEBNext Ultra II DNA Library Prep Kit for Illumina" (E7645) or the "NEBNext Ultra II FS DNA Library Prep Kit for Illumina" (E7805) (New England BioLabs). Sequencing was conducted on an Illumina MiSeq System (Illumina Inc.) at the Transcriptome and Genome Analysis Laboratory (University of Goettingen). Pools were mixed equimolarly and sequenced in two different paired-end runs (six pools, 24 samples each) with a 2 × 250-bp (500 cycles) version 2 kit (see Appendix S1 for details on library preparation).

2.4 | Read processing und alignment

We checked the quality of raw reads with FASTQC (available at: http://www.bioinformatics.bbsrc.ac.uk/projects/fastqc). Further processing of the raw reads was done using the pipeline HYBPHYLOMAKER (Fér & Schmickl, 2018). Sequence adapters were removed, and reads were quality-trimmed using TRIMMOMATIC version 0.32 (Bolger, Lohse, & Usade, 2014), with the default settings used in HYBPHYLOMAKER. Duplicated reads were removed with FASTUNIQ version 1.1 (Xu et al., 2012). Quality-trimmed individual raw reads were mapped to a reference sequence and then merged into contigs that are aligned for each gene separately. As pseudoreference for read mapping, we used a sequence consisting of the concatenated target exonic sequences, separated by stretches of 800 Ns. Mapping to the pseudoreference genome was done with BWA (Li & Durbin, 2009), and consensus sequences of the mapped reads were produced with CONSENSUSFIXER (available at: https://github.com/cbg-ethz/ConsensusFixer), because this is the only approach available in HYBPHYLOMAKER able to call ambiguity DNA codes in case of multiple bases per site in the mapped reads. For CONSENSUSFIXER we used the following settings: minimum relative abundance of the alternative base ("plurality" in the setting file of HYBPHYLOMAKER) of 0.2 and a minimum read coverage for ambiguity calling ("mincov") of 5.

Consensus sequences were matched to sequences of the target exons to produce PSLX files using BLAT (Kent, 2002). They were

therefore combined to produce exon-wise matrices with "assembled_exons_to_fastas.py" (Weitemier et al., 2014). Matrices were aligned with MAFFT version 7.029 (Katoh & Standley, 2013), using the default program settings, and then gene-wise concatenated with AMAS (Borowiec, 2016). We filtered potential paralogues by running the script "HybPhyloMaker4a2_selectNonHet.sh" and setting the maximum number of heterozygous sites per locus ("maxhet" in the HYBPHYLOMAKER settings file) to 10. We continued the pipeline with both data sets, filtered and unfiltered. HYBPHYLOMAKER performs two consecutive steps of missing-data filtering. First, sequences with more than a certain percentage of Ns in an alignment ("missing-percent" in the settings file) are deleted. We set this option to 40. Secondy, alignments with less than a certain per cent of sequences ("speciespresence" in the settings file) are filtered out. We set this value to 75, so that alignments with more than 25% of missing sequences (i.e., with fewer than 25 sequences) were excluded. Finally, we calculated alignments statistics for the selected genes with AMAS, TRIMAL version 1.2 (Capella-Gutiérrez, Silla-Martínez, & Gabaldón, 2009) and MSTATX (https://github.com/gcollet/MstatX/), as implemented in HYBPHYLOMAKER.

2.5 | Phasing

Because the importance of retrieving allele information for a correct phylogeny estimation (especially in a recently diverged group) has been emphasized in recent studies (Andermann et al., 2019; Eriksson et al., 2018), we tested the impact of allele phasing on our phylogenetic analyses. To avoid the loss of allelic information during the process of allele mapping and consensus sequence production, we extracted the.bam files produced after mapping the reads to the pseudoreference sequence from the HYBPHYLOMAKER pipeline. These were phased with SAMTOOLS version 0.1.19 (Li et al., 2009), using the combination of the commands "samtools sort" and "samtools phase." The phased.bam and.bai files were then placed in a new HYBPHYLOMAKER working directory for further processing within the pipelines workflow. A new "/10rawreads/" folder was also placed in the HYBPHYLOMAKER working directory, containing only the file with the modified sample names. The pipeline was therefore resumed for computing of the consensus sequences (this time allele-wise consensus sequences) by calling the script "HybPhyloMaker2_read-mapping.sh" but specifying "mapping = no" in the setting file. The alignments obtained are hereafter called allele alignments. We ran the pipeline further as explained above, with the only differences that (a) matrices of exons belonging to the same gene were not concatenated; and (b) exon trees (instead of gene trees) were inferred and used for further analyses.

2.6 | Position filtering

We evaluated the effect of filtering alignments for positions that could add phylogenetic noise to the phylogenetic reconstructions, the so-called "phantom" spike positions (ambiguous positions, usually situated close to indel-rich regions of the alignment, with abnormally high substitution rates). We followed the procedure illustrated by Fragoso-Martínez et al. (2017), calculating first the Phylogenetic Informativeness (Townsend, 2007) and net Phylogenetic Informativeness profiles using HYPHY (Pond, Frost, & Muse, 2005) in the web portal PhyDesign (López-Giráldez & Townsend, 2011). As tree inputs, we used trees (different trees for different data sets; consensus or allele alignments, paralogure filtering or not, etc.) obtained from HYBPHYLOMAKER by concatenating gene alignments and FASTTREE (Price, Dehal, & Arkin, 2010). The phylograms were then transformed to ultrametric trees using Penalized Likelihood methods (Sanderson, 2002) as implemented in the R package "ape" (Paradis & Schliep, 2018), with correlated rates and smoothing parameter (λ) set to 1. The relative timescale was set to 1 at the root.

Second, we used the estimated substitution rate per locus from HYPHY and the R script from Fragoso-Martínez et al. (2017) to identify the specific positions in the alignments with an unusually high substitution rate. As substitution rate threshold, we use 20 (the highest value tried in Fragoso-Martínez et al. (2017)) because we were just interested in deleting poorly aligned positions and artefacts, without running the risk of excluding naturally highly variable regions in the alignments. Detected sites were checked and removed manually from the alignments. Lists of the removed sites for each scenario are given in Table S2. The cleaned alignments were then reintroduced in the HYBPHYLOMAKER pipeline, just before the missing-data filtering step.

2.7 | Gene tree and species tree/network analyses

For all different data sets, species trees were estimated (a) using maximum likelihood (ML) as implemented in RAXML version 8.2.4 (Stamatakis, 2014) on the concatenated data sets (concatML) and (b) applying the coalescent-based method ASTRAL-III (Chao, Rabiee, Sayyari, & Mirarab, 2018). For the concatML analyses, concatenated alignments were produced in HYBPHYLOMAKER using AMAS and saved in PHYLIP format. Analyses were run on the Scientific Computer Cluster of the GWDG (https://www.gwdg.de/) using RAXML, with alignments partitioned by genes, the GTRGAMMA model and 100 bootstrap replicates. Concatenated analyses were only performed for the consensus alignments, because there was no way of knowing how the phased alleles of a sample combined across loci. We also quantified branch support and conflict on the concatML trees with the Quartet Sampling method (Pease, Brown, Walker, Hinchliff, & Smith, 2018).

For the coalescent-based analyses, first gene trees (or exon trees in the case of the allele alignments) were reconstructed with RAXML. Analyses were run with 100 standard bootstrap replicates, with the GTRGAMMA model and partitioning by exons. Gene tree characteristics (average bootstrap support, average branch length, etc.) and correlations among alignments and gene tree characteristics were calculated and plotted in R version 3.5.2 (R Core Team, 2018), using modified scripts from Borowiec (2016) as implemented

in HYBPHYLOMAKER. Gene trees were rooted, collapsing branches with bootstrap values <50, and combined into single NEWICK files using Newick Utilities (Junier & Zdobnov, 2010). Species trees were inferred applying the coalescent-based algorithm implemented in ASTRAL-III version 5.6.3 (Chao et al., 2018) with 100 multilocus bootstrap replicates. To assess the amount of gene tree conflict on branches, we measured the quartet support on the ASTRAL trees (Sayyari & Mirarab, 2016) for the main, the first alternative and the second alternative topologies ("-t 8" option in ASTRAL).

In addition, and to test for the extent of reticulate evolution among the sexual representatives of the *R. auricomus* complex, we inferred neighbor-net networks on the concatenated data sets using SPLITSTREE version 4.14.6 (Huson & Bryant, 2006). We used the General Time Reversible (GTR) model to estimate the genetic distance with estimated site frequencies and maximum likelihood (equal rates of site variation). Support values were calculated based on 100 bootstrap replicates.

2.8 | Divergence time estimation

To obtain absolute divergence times, we used two secondary calibration points for the analyses. The crown age of the *R. auricomus* complex was set according to Hörandl (2004). In this study, the divergence time between *R. notabilis* and *R. carpaticola* was estimated as 914,000 years, whereas the split between *R. notabilis* and *R. cassubicifolius* was 535,000 years. Consequently, we applied a normally distributed time to the most recent common ancestor (TMRCA) prior to the crown age of the complex, with prior distribution ranging between the two age estimates (0.7245 ± 0.189 milion years ago [Ma]). The root of the tree (only analysis including the outgroup; see below) was calibrated according to the dated phylogeny published in Emadzade and Hörandl (2011). Therefore, we used a normally distributed TMRCA prior for the root centred at 12.53 Ma (±2.3 Ma).

Divergence times were estimated with BEAST version 2.5.2 (Bouckaert et al., 2019) using the 50 gene alignments with the highest number of parsimony-informative (PI) sites from those of the consensus data set, without paralogue filtering and cleaned from "phantom spikes." Prior to analyses, the selected loci were tested for selection using an ad-hoc test based on dN/dS values. For the scope, we set the correct reading frame for each alignment using the script "HybPhyloMaker4b_correctframe_translate.sh" in HYBPHYLOMAKER and setting the maximum number of stop codons to 1. Therefore, we calculated gene-wise ω (dN/dS ratios) with codeML (implemented in PAML version 4.8; Yang, 2007), using the corrected alignments and the concatML as species tree. We did not find any genes showing signal of positive selection (which would have been excluded from further analyses; Tables S3 and S4).

We estimated the best fitting substitution model for the selected loci (Table S5) using the Bayesian Information Criterion (BIC) in JMODELTEST version 2.1.10 (Darriba, Taboada, Doallo, & Posada, 2012). Input files for the BEAST analysis were prepared in BEAUTI version 2.5.2 (Bouckaert et al., 2019). We used the *BEAST template and unlinked substitution models, clock models and gene trees for all loci. A strict clock was enforced and the average clock rate for one random locus was fixed to 1.66×10^{-6} while estimating all other clock rates in relation to this locus. We opted for adding an informative prior on the clock rate given the broad interval used for the calibration priors and because estimations based on isozyme data and the general clock used in Hörandl (2004) might not have been sufficiently accurate. The clock rate was derived from standard substitution rates for plant nuclear genes as in Pellino et al. (2013). Assuming a standard substitution rate of 5e-9 (Wolfe, Gouy, Yang, Sharp, & Li, 1989) and a generation time of 3 years for members of the *R. auricomus* complex (Pellino et al., 2013), the BEAST clock rate translates to 1.66e-6 mutations per thousand years. Formerly described species were treated as independent lineages. Tetraploid accessions of *R. cassubicifolius* were treated separately from the diploid representatives of the species.

Because the main goal of the analyses was to estimate the time frame of speciation events, and because these analyses were based only on a reduced number of loci, we used a soft-constrained approach on the species tree topology in order to reach faster convergence and to make the topology of the *BEAST tree similar to the topology of the species trees obtained with the other methods. In particular, the monophyly of the clade with the Illyrian taxa was enforced.

Substitution models for each locus were adjusted to those found with JMODELTEST, and the Birth–Death model was used as prior on the species tree. Two independent analyses were run for 2×10^9 generations, sampling every 100,000th generation. Effective sample size (ESS) values and convergence between independent analyses were checked in TRACER version 1.6 (Rambaut & Drummond, 2007). Results of the two analyses were merged using LOGCOMBINER version 2.5.2 (Bouckaert et al., 2019) applying a burn-in of 10%. Finally, the remaining 18,000 trees were used to construct a maximum clade credibility tree with a posterior probability limit set to 0.5 and "Mean Heights" for node heights using TREEANNOTATOR version 2.5.2 (Bouckaert et al., 2019). Another set of analyses was performed as described above, but including only the ingroup taxa, as many authors have highlighted that using outgroups in coalescent-based analyses violates some of the model assumptions (Agudo, Tomasello, Àlvarez, & Oberprieler, 2017; Drummond & Bouckaert, 2015).

An additional set of analyses was performed for the above-mentioned data sets (including and excluding the outgroup) using only clock rates or calibrations (and then applying an exponential prior with mean equal to 0.01 for clock rates) to obtain absolute time estimates. This was done to evaluate the effect of using both calibration and clock rate priors in the same analysis, and to test for congruence of the resulting time estimates.

2.9 | Ancestral area reconstruction

To evaluate hypotheses about past distribution patterns and dispersal and/or vicariance events in the evolutionary history of the

sexual representatives of the *R. auricomus* complex, we performed an ancestral area reconstruction with the R package BIOGEOBEARS version 1.1.2 (Matzke, 2018). This approach allows several models of biogeographical evolution to be compared via likelihood-based model selection (Matzke, 2013). Because sexual *R. auricomus* species grow within or near the main European mountain ranges, we assigned them to the seven following areas: Northern Carpathian (A), Southern Carpathian (B), Illyrian region (at the edge of the southeastern border of the Alps; C), Northern Prealps (D), Central Apennines (E), Massif Central (F) and Pyrenees (G; Figure 1). As tree input, we used the *BEAST tree without the outgroup taxa, because use of widely distributed and nonuniformly sampled outgroups would have been counterproductive for the analyses. We specified a distance matrix (including scaled geographical distances among predefined areas), and activated the *x* parameter, which can be used to estimate dispersal probability as a function of distance (Van Dam & Matzke, 2016). Ancestral areas were estimated under all six available models DEC, DIVA-LIKE and BAYAREA-LIKE, with and without the jump-dispersal parameter *j*. We compared the different nested models (e.g., DEC + *x* against DEC) with a likelihood ratio test (LRT) and selected the overall best-fitting model using the Akaike Information Criterion (AIC).

3 | RESULTS

3.1 | Gene capture and sequencing

The average number of obtained reads per sample was 1,373,158 (range 867,000–to 2,178,952). Read quality was relatively high, and on average only 3.27% of reads per sample were discarded after quality check (Table S6). The average per cent of mapped reads was 70.14%, with mapping success ranging from 53% to 82%, and only one sample (*Ranunculus notabilis* s.l.; 2) exhibiting a considerably lower number of mapped reads (26.89%; Table S7). Mapping success was not taxon-dependent. The sample with the highest mapping per cent belongs to the outgroup (*R. pygmaeus*, 82.48%). From the initial 736 target loci, 700 were successfully captured. On average, 612 loci per sample were captured, with LH008-7 (*R. cassubicifolius*) capturing the most (621 loci), and *R. sceleratus* the least (595 loci).

3.2 | Alignments and the impact of the different filtering schemes

The number of alignments used for the phylogenetic analyses varied according to the filtering scheme applied (Table 2). For the "consensus data set," about 15% of loci were excluded after missing data filtering and more than 25% after paralogue filtering (more than 50% of the total alignment length). Concerning the "allele alignments," working with exons made it possible to retrieve more loci (more than 80% and 50% of the total alignment length before and after paralogue filtering, respectively). More details are given in Table 2.

Allele phasing generated alignments with a considerably higher proportion of PI sites compared to the consensus alignments (5.82% and 1.4% on average, respectively). Paralogue filtering resulted in a loss of a fraction of PI sites in both the consensus and the allele data sets. When selecting the 50 loci for the BEAST analyses, 14.02% (78,458 bp) of the total matrix length was retrieved, comprising >23% of the total PI sites (1,971). Lists of the alignments used in the different filtering schemes, their characteristics and substitution models of the loci selected for the BEAST analyses are given in Table S5.

3.3 | Phylogenetic analyses and species trees

Species trees obtained from the concatML and coalescent-based analyses of the consensus data set showed topological incongruences across most of the filtering scenarios. When using allele alignments, coalescent-based species trees obtained from different filtering treatments always showed the same topology, differing only slightly in support values and branch lengths. When taking the average local posterior probability (LPP) of the ASTRAL bootstrap trees as a criterion to compare different treatments, the paralogue filtering tool offered in HYBPHYLOMAKER significantly worsened the results (in a post-hoc Tukey's test only differences between treatments with and without paralogue filtering were significant; Table S8), whereas position filtering improved support values slightly in some cases (Figure S1). No significant differences were noticed between "consensus" and "allele" data sets. Accordingly, and as a matter of simplicity, only results of the "consensus" and "allele" analyses, without paralogue filtering and with position filtering, are shown in Figures 2 and 3. The rest of the trees are available as Figures S2–S7.

We detected two main incongruences among species trees. (a) The position of the taxa within *R. notabilis* s.l. This clade is always highly supported, and in general samples cluster according to the taxonomy proposed by Dunkel et al. (2018), with the exception of "*R. austroslovenicus*" and "*R. calapius*" that in some cases are found to be polyphyletic. However, support values are usually low within the clade and phylogenetic relationships among taxa change consistently across analyses. (b) The position of *R. marsicus*, which often forms a clade with *R. envalirensis* s.l. but is resolved as sister to *R. flabellifolius* in some analyses. Support values of these phylogenetic relationships are generally low and branches very short.

Apart from these considerations, relationships among the main clades in the *R. auricomus* group are constant across analyses. The first split separates *R. cassubicifolius* s.l. from the rest of the taxa. The tetraploid *R. cassubicifolius* was well separated from the diploid accessions of the same species. In general, samples do not seem to cluster according to geographical origin within this clade. In the other main clade, samples cluster according to geographical distribution. *R. flabellifolius* (Southern Carpathians) occupies a basal position, whereas the clade with samples from the Massif Central and the Pyrenees (*R. envalirensis* s.l.) is sister to the Illyrian clade. The position of the Apenninian *R. marsicus*, as mentioned above, is equivocal. The same patterns can be found in the Neighbor-net results

TABLE 2 Alignment characteristics and performance of different filtering scenarios for the consensus and the allele data set

		Missing-data filtering			
				Paralogue filtering	
	Initial		Position filtering		Position filtering
Consensus					
Loci (exons)	700 (2,628)	605	605	521	521
Total length	727,475	562,824	559,781	302,963	301,868
Average proportion of PI sites	0.0145	0.0151	0.0152	0.0127	0.0127
Average LPP ASTRAL trees		0.776 (0.223)	0.776 (0.225)	0.728 (0.238)	0.729 (0.239)
Allele					
Loci (exons)	700 (2,628)	663 (2,495)	662 (2,493)	588 (1,815)	587 (1,813)
Total length	728,903	597,424	595,772	372,948	371,426
Average proportion of PI sites	0.0585	0.0611	0.0611	0.0553	0.0553
Average LPP ASTRAL trees		0.770 (0.229)	0.767 (0.227)	0.736 (0.239)	0.735 (0.239)

Note: For the Local Posterior Probability (LPP) of the ASTRAL bootstrap trees, mean values are given with standard deviation in parentheses.

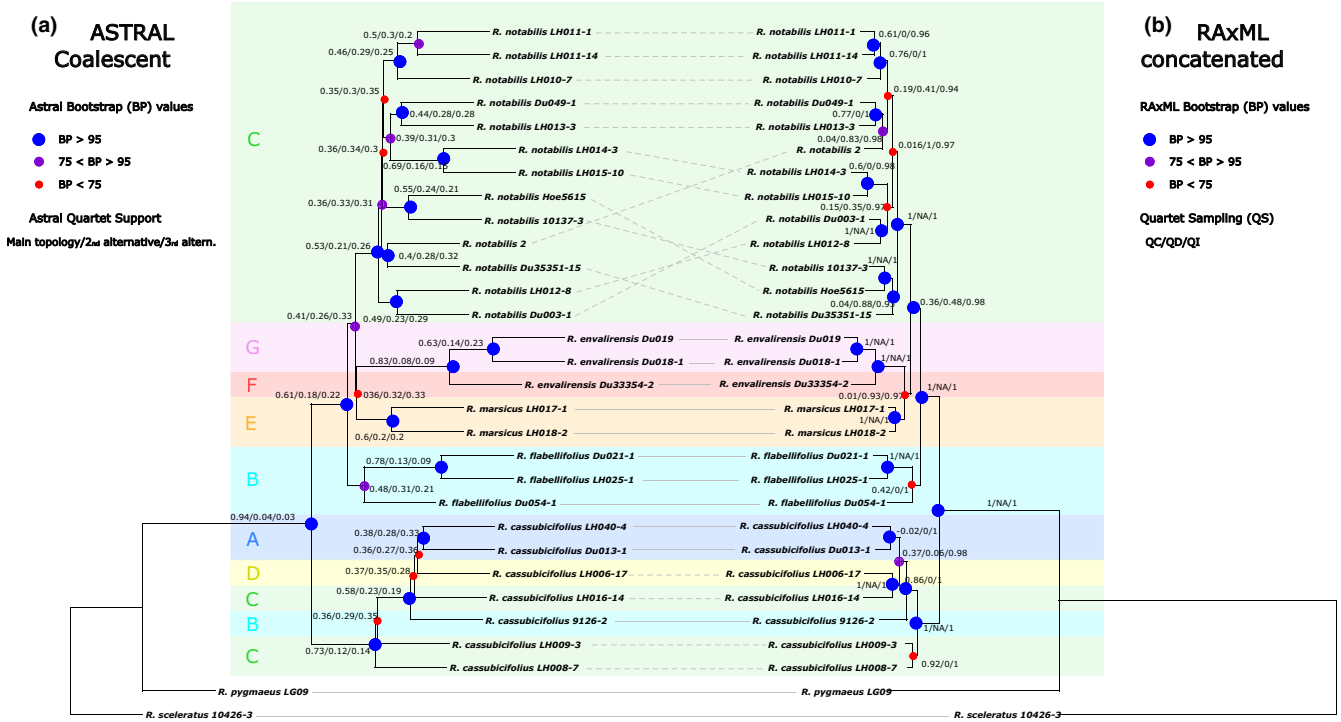

FIGURE 2 Tanglegram showing the coalescent-based ASTRAL species tree (a) and concatenated maximum likelihood tree (b), based on the consensus data set after applying position filtering and without paralogue filtering. Continuous lines indicate accessions with a congruent position, and dashed lines indicate incongruence. Circles on the nodes refer to bootstrap support values. Blue big circles are for support values above 95, purple medium-sized circles are for values between 75 and 95, and small red circles are for values below 75. Numbers at nodes indicate ASTRAL quartet support values (a) and quartet sampling results on the maximum likelihood tree (b). Colours and letters refer to the areas defined for the ancestral range reconstruction, as indicated in Figure 1

(Figure S8), which indeed do not support substantial reticulate evolution among sexual taxa of the *R. auricomus* complex. In these analyses, clusters formed by samples of *R. marsicus* do not receive high bootstrap support.

3.4 | Age estimation

Results from the two *BEAST analyses (including and excluding the outgroup) were congruent to a large extent, varying only slightly on the age

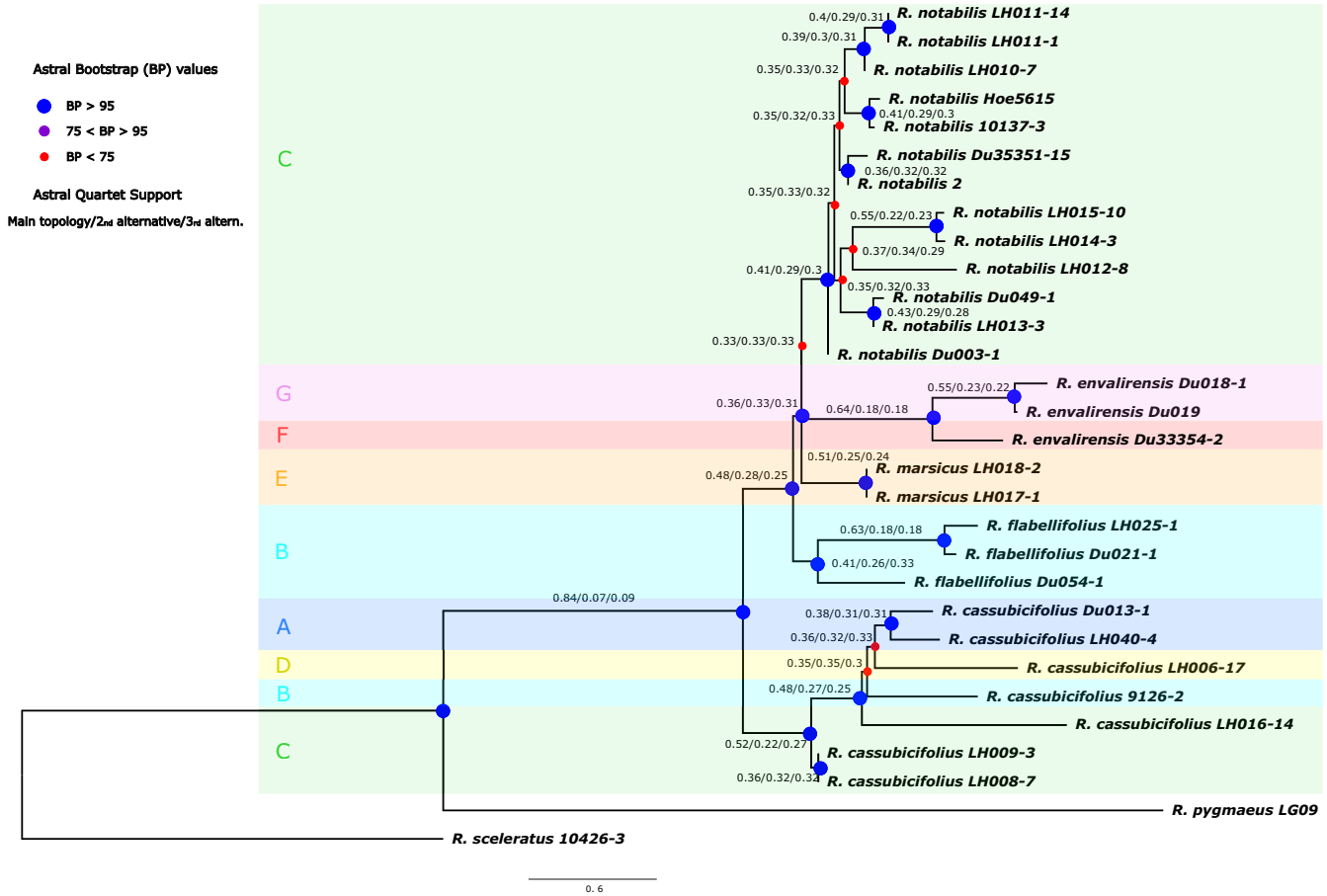

FIGURE 3 ASTRAL species tree based on the allele data set after applying position filtering and without paralogue filtering. Circles on the nodes of the trees refer to bootstrap support values. Blue big circles are for support values above 95, purple medium-sized circles are for values between 75 and 95, and small red circles are for values below 75. Numbers at nodes indicate ASTRAL quartet support. Colours and letters refer to the areas defined for the ancestral range reconstruction, as indicated in Figure 1

estimates. As for the concatML and the ASTRAL species tree, relationships within *R. notabilis* s.l. and within *R. cassubicifolius* s.l. are blurred and phylogenetic relationships receive low support (Figure 4; Figure S9).

The crown age of the *R. auricomus* complex is estimated to be ~733.5 thousand years ago (ka) (Table 3), somewhat older (~750 ka) in the analyses including outgroups (Figure S9). Most of the speciation events occurred between 830 and 580 ka. The only exception is the Apenninian *R. marsicus*, which diverged from *R. notabilis* s.l. more recently (266–107 ka). However, the latter result does not seem to be supported by the concatML and by the species tree analyses, in which *R. marsicus* is rather found to be related to *R. envalirensis* (but see support values in Figures 2 and 3), and its divergence seems to have occurred much earlier. Results of analyses including only calibrations or clock rates were congruent to those of the main analyses (Table S9).

Differentiation within *R. notabilis* s.l., *R. envalirensis* s.l. and *R. cassubicifolius* s.l. occurred in the last 200 thousand years, with the crown ages of these three species estimated as 176, 147 and 130 ka, respectively (166, 128 and 119 ka in the analysis including outgroups; Figure S9).

3.5 | Ancestral area

The LRT shows that results of models including the *x* parameter were significantly better ($p < .05$) than those without this parameter (Table S10). The *j* parameter did not improve the model fit for DEC and DIVA-LIKE, whereas it considerably ameliorated the BAYAREA-LIKE model fit. Overall, the best-fitting model was the DIVA-like + *x* (Table 4).

Results of the DIVA-LIKE + *x* model support a vicariance scenario, with the existence of a widespread ancestor for the *R. auricomus* complex (Figure 5a). The most probable ancestral range of *R. cassubicifolius* s.l. was the Northern Carpathians and the Northern Prealps, while the ancestor of the remaining species most probably had a southern range, being distributed in the Southern Carpathians, Apennines and Pyrenees. However, some uncertainty is present in the estimation of the ancestral areas for the deepest nodes of the phylogeny, and statistical differences between the most probable and alternative ancestral ranges are relatively low for some nodes (Figure 5b).

4 | DISCUSSION

4.1 | Phylogenetic relationships among sexual species of the *R. auricomus* complex

Disentangling phylogenetic relationships among recently and rapidly diverged lineages remains a challenge (Knowles & Chan, 2008). In the present study, we resolved the phylogeny of the sexual representatives of the less than 1-Myr-old *Ranunculus auricomus* complex. To this end, we analysed Target Enrichment data using concatenated ML and coalescent-based species-tree inference methods. Target Enrichment is considered to be a very suitable approach for resolving deep phylogenies, as the baits are usually designed for highly conserved regions (McCormack et al., 2013; McKain, Johnson, Uribe-Convers, Eaton, & Yang, 2018). Nevertheless, the potential of this method for resolving shallow phylogenies and application in population genetic studies has been highlighted recently (Harvey, Smith, Glenn, Faircloth, & Brumfield, 2016). Until now, this sequencing approach has been applied a few times to resolve phylogenetic relationships in recently radiating plant and animal groups (e.g., the 7.2-Myr-old genus *Heuchera* [Folk, Mandel, & Freudenstein, 2015]; the ~3-Myr-old carnivorous plant *Sarracenia* [Stephens et al., 2015]; the rapid island radiation of the Philippine Shrews [<4.8 Ma; Giarla & Esselstyn, 2015]; and the lizard species group *Liolaemus fitzingerii* [2.6 Ma; Grummer, Morando, Avila, Sites, & Leaché, 2018]). The crown age of the *R. auricomus* complex was estimated to be 733.5 ka (829–639 ka) herein. In this sense, our study represents the most outstanding example of employing Target Enrichment data in recently and rapidly radiating species complexes.

The main problems when working with rapidly radiating groups are: (a) rampant incomplete lineage sorting (ILS) due to the fact that ancestral polymorphisms are carried through a series of nearly simultaneous speciation events; and (b) the lack of information due to the slow mutation rate of the (most often) coding regions used in studies employing a Target Enrichment approach (Giarla & Esselstyn, 2015). Using information from several (hundreds of) independent loci from multiple individuals per species, and applying coalescent-based species tree methods should improve phylogenetic

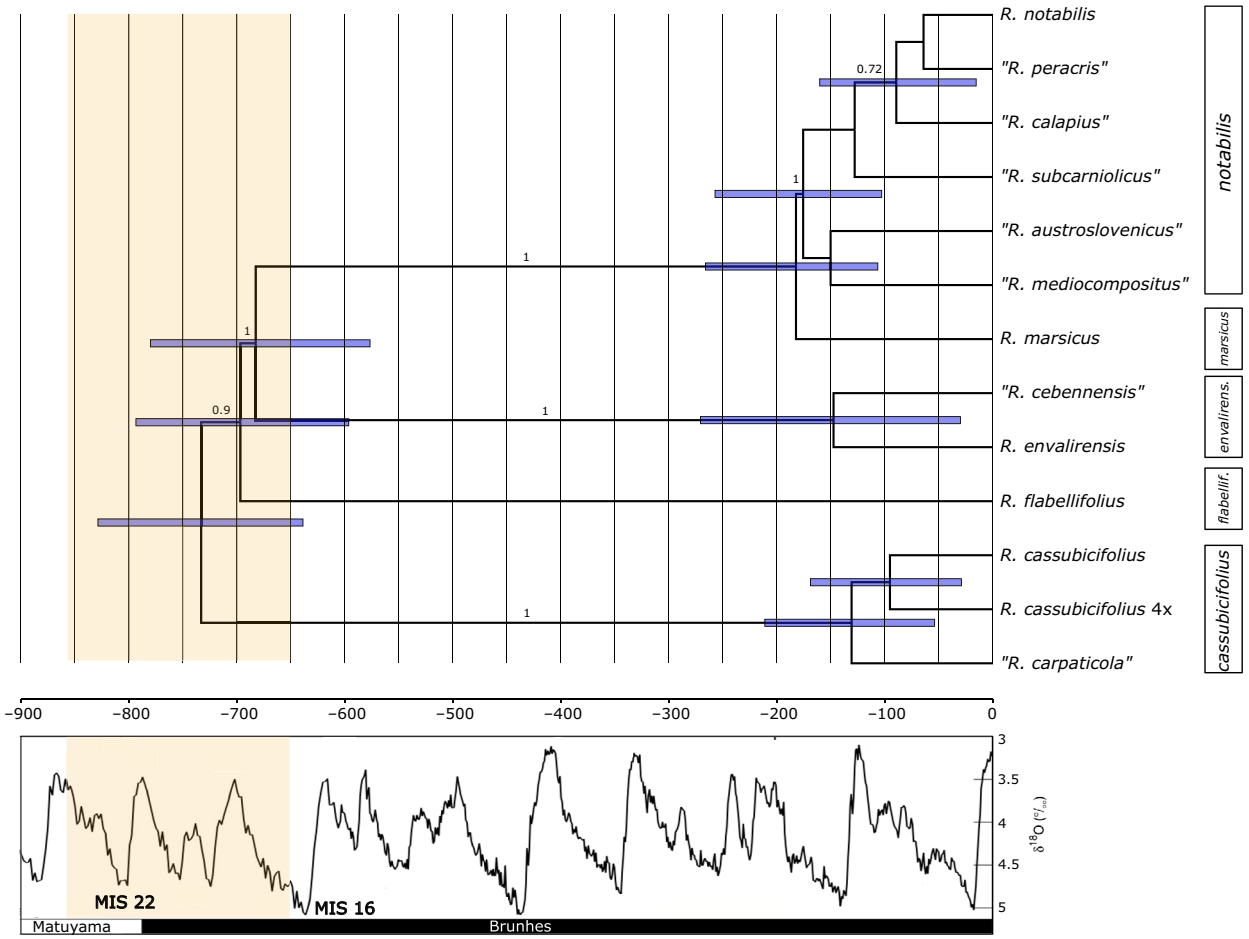

FIGURE 4 Maximum clade credibility tree estimated in *BEAST using the 50 most informative loci from the consensus data set. Blue bars indicate 95% highest posterior density (HPD) intervals of the age estimate (see Table 3). Numbers above branches indicate Bayesian posterior probabilities; only values above 0.7 are shown. On the right, bars indicate the current nomenclature according to Karbstein et al. (2020). The curve below the tree represents the $\delta^{18}O$ modified from Lisiecki and Raymo (2005). Valleys correlate with cold periods (glaciations) and peaks with warm periods (interglacials). Marine Isotope Stages (MIS) 22 and 16, representing the two most severe glaciations during the Mid-Pleistocene Transition (MPT), are also indicated. The orange region corresponds to the final phase of the MPT

TABLE 3 Prior and posterior distributions of age estimates (ka) for the most important nodes of the *BEAST chronogram for *Ranunculus* (Figure 4)

	Prior distribution		Posterior distribution	
Node description	Median age	95% HPD interval	Mean age	95% HPD interval
Root	724.5	914–535	733.5	829.1–639.2
R. flabellifolius stem age			697.2	793.9–596.8
R. envalirensis clade stem age			683	780.6–577.1
R. marsicus–*R. notabilis* s.l. split			182.5	266.3–106.7
R. notabilis s.l. crown age			175.9	257.5–103.1

Abbreviation: HPD, highest posterior density.

TABLE 4 Summary of data likelihoods under each model, and results of statistical model choice

Model	Max. no. of areas	LnL	No. of parameters	*d*	*e*	*x*	*j*	AIC
DEC	7	−26.228	2	0.210	0.497	—	—	56.457
DEC + *x*	7	−22.757	3	2.275	1E-12	−2.020	—	51.513
DEC + *j*	7	−24.274	3	0.063	1.0E-12	—	0.054	54.548
DEC + *x* + *j*	7	−22.597	4	1.213	1.0E-12	−1.736	0.210	53.195
DIVA	7	−21.475	2	0.123	1.0E-12	—	—	46.950
DIVA + *x*	**7**	**−18.307**	**3**	**0.890**	**1.0E-12**	**−1.522**	—	**42.614**
DIVA + *j*	7	−21.473	3	0.121	1.0E-12	—	0.002	48.946
DIVA + *x* + *j*	7	17.718	4	2.450	1.0E-12	−2.243	1.0E-05	43.437
BAYAREA	7	−31.872	2	0.278	2.791	—	—	67.744
BAYAREA + *x*	7	−29.506	3	2.976	2.911	−1.771	—	65.012
BAYAREA + *j*	7	−26.982	3	0.059	0.536	—	0.063	59.963
BAYAREA + *x* + *j*	7	−25.354	4	0.336	0.218	−1.253	0.302	58.709

Note: Estimates for the parameters dispersal parameter (*d*), extinction (*e*), *x* (dispersal probability as a function of distance) and *j* (jump speciation events at cladogenesis). The favoured model is in bold type.

inference and overcome the above-mentioned problems (Kumar, Filipski, Battistuzzi, Pond, & Tamura, 2012). However, in Grummer, Morando, Avila, Sites, and Leaché (2018) even 580 loci were not enough to provide significant support for interspecific relationships in the *L. fitzingerii* species group. In *R. auricomus*, 500–600 loci were able to resolve phylogenetic relationships among the main lineages of the complex. Incongruence was found mostly within the Illyrian group and within the clade of *R. cassubicifolius* s.l. There, relationships among formerly described species were inconsistent across analyses and clades did not receive significant support, confirming the broader species delimitation provided by Karbstein et al. (2020). Diversification processes within these two species (i.e., *R. notabilis* s.l. and *R. cassubicifolius* s.l.) took place recently and in a very short time frame (i.e., the last 176 and 136 kyr, respectively). We believe that the lack of phylogenetic divergence might be the cause of the poorly resolved intraspecific relationships in these two species. As already observed in comparable complexes (Grummer et al., 2018; Stephens et al., 2015, for organellar genomes), there might have been too little time for the genomes to accumulate enough informative polymorphisms.

When looking at the backbone of the phylogenetic trees, the main source of incongruence is the tetraploid *R.marsicus*, which exhibits inconsistent positions in different concatML analyses, and in the ASTRAL and *BEAST species trees. However, all these sister relationships are not supported and the branches describing them are usually very short. Possible causes of these contrasting patterns can be either ILS or hybridization/introgression. An allotetraploid origin of *R.marsicus* with the parental contribution of ancestral relatives of *R.notabilis* and *R.envalirensis* might be a realistic and geographically plausible scenario, and STRUCTURE analyses based on RADseq data in Karbstein etal.(2020) seem to support it to some extent. However, in the present analyses, the high quartet differential values of the quartet sampling (for the concatML; Figure2), and the comparable frequencies of the two alternative topologies in the quartet support of the ASTRAL trees, sustain the hypothesis of ILS as the cause of incongruence rather than hybridization (Figure3; FiguresS2–S7). Our Neighbor-net analyses do not support an allopolyploid origin of *R.marsicus* with the contribution of ancestral relatives of *R.notabilis* and *R.envalirensis*. In these analyses, *R.marsicus* seems to occupy a more basal position between *R.flabellifolius* and *R.envalirensis*, and no

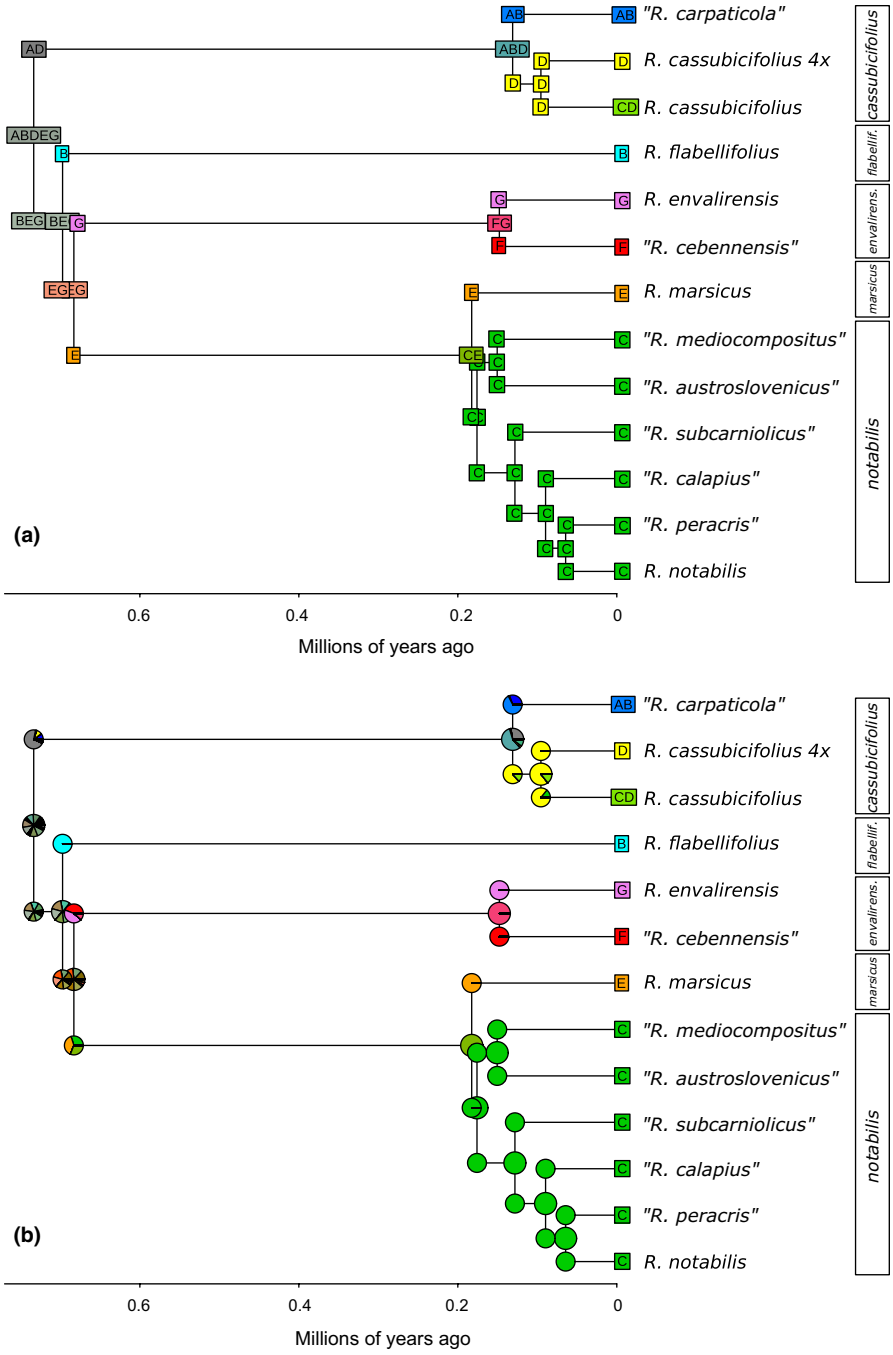

FIGURE 5 (a) Ancestral state reconstruction for the sexual representatives of the *Ranunculus auricomus* complex, as estimated in BIOGEOBEARS using the favoured DIVALIKE + *x* model. (b) Plot of the single-most-probable geographical range at each node (just before speciation) and post-split (just after speciation). Pie charts represent the probabilities of each possible geographical range per node. Capital letters indicate the areas defined for the analysis: A, Northern Carpathians; B, Southern Carpathians; C, Illyrian region; D, Northern Prealps; E, Central Apennines; F, Massif Central; and G, Pyrenees. Bars to the right of the diagrams indicate the species delimitation according to Karbstein et al. (2020)

significant signal of reticulation can be observed. The two scenarios (ILS or reticulation producing incongruence in the data set) are not necessarily mutually exclusive and a definitive and unequivocal reconstruction of the processes giving rise to this polyploid taxon, which requires a different experimental design and more specific analyses (e.g., coalescent-based species network inference), is far beyond the scope of the present study.

Concerning differences among tree inference methods (concatenated vs. coalescence-based) and performance of data sets from different filtering settings, we note that concatenation usually resulted in higher bootstrap values (compared to equivalent coalescent-based analyses) even though topologies were more discordant among trees. Similar patterns have already been observed in empirical and simulation studies (Herrando-Moraira & The Cardueae Radiations Group, 2018; Kubatko & Degnan, 2007; Weisrock et al., 2012). Remarkably, trees obtained by applying coalescent-based analyses to the phased data set were topologically identical, and minor differences concerned only branch lengths and support values (Figures S5–S7). This is further evidence that using allelic information together with coalescent-based species tree approaches can considerably increase the trustworthiness of phylogenetic analyses (Andermann et al., 2019). Concerning the performance of different phasing and filtering settings, the paralogue filtering implemented in HYBPHYLOMAKER significantly worsened branch supports. Applying this option to diploids possibly resulted in the elimination of many nonparalogue (but variable) alignments. Moreover, paralogy might

not be an issue in our data set, because the baits kit was specifically designed for members of the *R. auricomus* complex. Therefore, it is rather unlikely that the selected single-copy regions went through duplication in some of these very closely related taxa. No significant amelioration in support values of the bootstrap ASTRAL trees was produced when applying phasing (but see above considerations on tree topologies) or position filtering (Figure S1).

4.2 | Time frame of diversification processes

The crown age of the *R. auricomus* complex was estimated to be ~730 ka (Table 3). Hörandl (2004) estimated the divergence time between three sexual species using isozyme allelic frequencies and genetic distances after Nei (1975). Ages of these divergence events were estimated to 914,000 and 535,000 years, respectively, even though they describe the same split in the phylogeny of the complex (the crown age of the whole group). Therefore, using a broad prior for the crown age of the complex and a relatively informative prior for the clock rate (according to the mutation rates estimated for the complex by Pellino et al., 2013), we were able to estimate the age of this node more precisely. Moreover, we obtained the time frame of all speciation events among sexual representatives of *R. auricomus*. Interestingly, almost all these events have taken place in a very short time between 830 and 580 ka (Figure 4). The only exception is the tetraploid species *R. marsicus*, which seems to have diverged much more recently (but see considerations about uncertainty above). The divergence estimates for all these speciation events coincide with the Mid-Pleistocene Transition (MPT; Clark et al., 2006; Lisiecki & Raymo, 2005), one of the most important climatic changes occurring in the Pleistocene. During this interval (1.2 Ma to 650 ka), the relatively low-amplitude 41-kyr climate cycles of the earlier Pleistocene were progressively replaced by high-amplitude 100-kyr cycles (Lisiecki & Raymo, 2005). Glaciations became longer and more severe, and the average global ice volume increased consistently, with larger increases at high and middle latitudes of Eurasia and North America (Elderfield et al., 2012; Raymo, Lisiecki, & Nisancioglu, 2006). This process became progressively stronger, and evidence from all northern continents indicates that Marine Isotope Stage (MIS) 22 (~870–880 ka) was the first of the major glaciation events characterizing the later Pleistocene (Head & Gibbard, 2005). At the end of the MPT (MIS 16; ~650 ka), the most substantial glaciation yet experienced in the northern hemisphere took place (Head & Gibbard, 2005). This tremendous climatic transition was probably the consequence of the increase in atmospheric moisture provided by warm subtropical water in the Western Mediterranean region that, combined with a decrease in boreal summer insolation, contributed to the feed of the ice-sheets in Central and Northern Europe (Bahr et al., 2018; Sánchez-Goñi et al., 2016). The onset of the global cooling phase and ice expansion caused a major restructuring of the global vegetation and faunal systems (Alroy, Koch, & Zachos, 2000; Gaboardi, Deng, & Wang, 2005; Zhao et al., 2017; Zhou et al., 2018).

Diversification processes within species took place more recently, most probably within the last two glaciation cycles. Diverging populations of *R. envalirensis* s.l., *R. notabilis* s.l. and *R. cassubicifolius* s.l. differentiated allopatrically (in the first case) or parapatrically (in the latter two cases) within the last 160 ka (Figure 4). As for the alpine taxa, and probably also for montane plant species, the last two glaciation cycles were a triggering force shaping intraspecific genetic patterns, but were not sufficiently long to complete speciation processes. Overall, our age estimates are concordant with those found in previous studies (Emadzade & Hörandl, 2011; Hörandl, 2004; Pellino et al., 2013). In Hörandl (2004) and Emadzade and Hörandl (2011), diversification processes within *R. cassubicifolius* were found to be slightly older, 317 and 640 ka, respectively. In our analyses, sexual autotetraploids in *R. cassubicifolius* (Hörandl & Greilhuber, 2002) were found to be ~95,000 years old. This result is in accordance with previous studies estimating the maximum age of hexaploid apomictic derivatives as 80,000 years (Pellino et al., 2013), and confirms the general assumption that the origin of polyploids is associated with the last glaciation cycle.

4.3 | Biogeographical history

In our biogeographical analyses, AIC preferred models supporting the existence of a widespread ancestor for the *R. auricomus* complex, stressing the importance of vicariance in triggering speciation events among sexual representatives of the complex (Table 4). The ancestor of the whole complex was reconstructed to be distributed in the whole of Europe, although with some uncertainty (Figure 5). A first vicariance event separated populations with a northern distribution (giving rise to *R. cassubicifolius* in the Northern Prealps and the Western Carpathians) from those with a southern distributional range. Further vicariance events then gave rise through allopatric speciation to the remaining sexual species of the complex (i.e., *R. flabellifolius*, *R. envalirensis*, *R. marsicus* and *R. notabilis*).

Almost all of these vicariance events occurred in a restricted period, coinciding with the final stage of the MPT. At the beginning of this period of drastic climatic change, humid and mild temperate forests with deciduous oaks and tertiary elements (such as *Carya* and *Zelkowa*) occupied a vast area of continental Europe (Magri & Palombo, 2013; Pastre et al., 2007; Stuchlik & Wójcik, 2001). Such environments must have been similar to the ecosystems inhabited nowadays by many of the sexual representatives of the complex. Climatic deterioration (the progressive cooling and drying of the climate) resulted in the fragmentation of such environments and the establishment of grass-dominated open vegetation adapted to cold and arid conditions (Magri & Palombo, 2013). Towards the end of the MPT, tundra vegetation was well established in Central and Northern Europe (Stuchlik & Wójcik, 2001). A similar situation was registered in temperate Eastern Asia, where broadleaved mixed forests dominated by *Quercus* and *Pinus* shrank significantly during the MPT, transforming into grass-dominated vegetation definitively by around 0.7 Ma (Zhou et al., 2018).

Areas at the foothills of mountain systems might have acted as microrefugia for species of deciduous temperate forest ecosystems. Indeed, for the boreomontane *P. verticillatum*, putative glacial refugia were identified in the area surrounding the glaciated Alps and in the foothills of the Carpathian and Balkan mountain systems (Kramp et al., 2008). The ancestor of the *R. auricomus* complex might have therefore inhabited the deciduous temperate forests widespread in Europe during the first phases of the MPT. Climatic deterioration and the retreat of temperate forests to isolated refugial areas efficiently separated *R. auricomus* populations, which finally gave rise to the different sexual species of the complex by allopatric speciation. A similar pattern of allopatric speciation in the Mid-Pleistocene was inferred for the temperate-montane Asian species *Dysosma versipellis* (Qiu, Guan, Fu, & Comes, 2009). Surprisingly, the sexual species of the *R. auricomus* complex did not show long-distance dispersal, which has been observed in many other plant genera (Knapp et al., 2005), and also in other forest species from other clades of the genus *Ranunculus* (Emadzade et al., 2011). The achenes as diaspores exhibit no obvious specialized structures potentially suitable for long-distance dispersal via anemo- or zoochory. The absence of long-distance dispersal in the sexual *R. auricomus* species may also reflect limited abilities to adapt to new environments or novel niches. Outcrossing and self-sterility in the diploids may be other reasons for low colonization abilities (Hörandl, 2008). Nevertheless, moderate range expansions in warmer periods between 600 and 200 ka should be considered, especially in the *R. cassubicifolius*, *R. envalirensis* and *R. notabilis* clades, as their respective crown group areas are larger than their stem group areas (Figure 5a). Such geodispersal during interglacials might have potentially resulted in secondary contact hybridization and an allopolyploid origin of the apomictic taxa. However, range expansions remained at a regional scale and did not allow sexual taxa to cover again the whole ancestral area of the *R. auricomus* complex. In fact, dispersal and vicariance scenarios are not mutually exclusive (Sanmartín, 2009).

A second wave of intraspecific vicariance occurred ~200–100 ka in the Alpine–Carpathian system (*R. cassubicifolius* s.l.), between the Pyrenees and the Massif Central (*R. envalirensis* s.l.) and, to a lesser extent, within the Illyrian clade (*R. notabilis* s.l.). Most taxa occur today disjunctly in very restricted areas with few populations, although appropriate habitats would be broadly available. The disjunct patterns suggest that survival of the last glacial periods occurred also in microrefugia where local conditions protected plant species from unfavourable regional conditions (Rull, 2009). A distribution pattern suggesting survival in proximal microrefugia is specifically apparent in *R. cassubicifolius* in the northern foothills and foreland of the Alps. Here, the species occurs today only in patchy areas that remained ice-free between the large glacier tongues of the Last Gacial Maximum (LGM; see map in Paun, Stuessy, & Hörandl, 2006).

Strikingly, the species are still distributed just in their very restricted areas, despite post-glacial reforestation of temperate Europe. The failure of the sexual species in post-glacial geodispersal may be explained by biotic barriers, namely congeneric competitors. The origin of polyploid apomictic derivatives is presumably younger than 100 thousand years (Pellino et al., 2013), and they rapidly colonized various habitats following the LGM (Paun et al., 2006). The rapid range expansion of younger, polyploid apomictic derivatives of the *R. auricomus* complex could have blocked range expansion of sexual progenitors (Hörandl, 2006). Polyploid apomicts could be more competitive, but they could also benefit from having no minority cytotype disadvantage (Levin, 1975): sexual outcrossers need a conspecific pollinator for reproduction, while the apomicts can reproduce as single individuals (Kirchheimer et al., 2018). Fertilization of sexual individuals by sympatric apomictic pollen donors can even result in the formation of aneuploid, introgressed offspring. Such processes were observed in diploid *R. notabilis* populations mixed with tetraploid apomicts (Hörandl, Greilhuber, & Dobes, 2000) and may also occur between sexual and apomictic cytotypes of *R. marsicus* (Dunkel, 2011). However, other distantly related and widespread species of the genus occupying the same habitats within the forest zone (e.g., *R. polyanthemos* group, or *R. lanuginosus*) could also have been competitors for sexual taxa of *R. auricomus*. *R. marsicus* and *R. envalirensis* established small populations in subalpine grassland habitats in the Apennines and Pyrenees, respectively. Here, members of the widespread, distantly related *R. montanus* group are very abundant (E. Hörandl, L. Hodač, pers. obs.) and are probably more successful. Hence, geographical parthenogenesis is resulting not only from the colonization success of apomicts, but also from failure of sexual species to expand ranges.

We conclude that biogeographical histories in temperate forest plants are complex, as area configurations changed over time due to climatic fluctuations. Vicariance, allopatric speciation and fragmentation of habitats during colder climatic periods shaped the evolutionary history of the sexual species of the *R. auricomus* complex. Our observations fit a hierarchical vicariance model (sensu Ronquist & Sanmartín, 2011). However, even after disappearance of climatic barriers after the LGM, biotic barriers of congeneric competitors might have blocked range expansions of sexual species of the *R. auricomus* complex.

ACKNOWLEDGEMENTS

We thank the German Research Foundation for project funding (DFG, Ho4395/10-1) to E.H., within the priority programme "TaxonOmics: New Approaches for Discovering and Naming Biodiversity" (SPP 1991), and the Botanical Museum, University of Oslo (O) for the material of *R. pygmaeus*. We also thank Mr F. G. Dunkel for providing herbarium vouchers and living material for the recently discovered diploid populations from the Illyrian region and France.

AUTHOR CONTRIBUTIONS

S.T. and E.H. conceived the ideas; S.T., K.K., L.H. and E.H. collected materials and data; S.T., K.K. and C.P. analysed the data; and S.T. wrote the paper with contributions from all co-authors.

DATA AVAILABILITY STATEMENT

The raw reads used in this study are deposited in the Sequence Read Archive (SRA) under the BioProject PRJNA628081.

ORCID

Salvatore Tomasello https://orcid.org/0000-0001-5201-1156
Kevin Karbstein https://orcid.org/0000-0003-1424-6557
Ladislav Hodač https://orcid.org/0000-0002-6885-1317
Claudia Paetzold https://orcid.org/0000-0002-4128-6645
Elvira Hörandl https://orcid.org/0000-0002-7600-1128

REFERENCES

Abbott, R., Albach, D., Ansell, S., Arntzen, J. W., Baird, S. J. E., Bierne, N., … Zinner, D. (2013). Hybridization and speciation. *Journal of Evolutionary Biology*, *26*, 229–246. https://doi.org/10.1111/j.1420-9101.2012.02599.x

Agudo, A. (2017). *Evolución en Anacyclus L. (Anthemideae, Asteraceae). Análisis de la zona de contacto entre A. clavatus (Desf.) Pers. y A. valentinus L.* (Unpublished doctoral dissertation). Universidad Autónoma de Madrid.

Alroy, J., Koch, P. L., & Zachos, J. C. (2000). Global climate change and North American mammalian evolution. *Paleobiology*, *26*, 259–288. https://doi.org/10.1017/S0094837300026968

Alsos, I. G. (2005). Impact of the ice ages on circumpolar molecular diversity: Insights from an ecological key species. *Molecular Ecology*, *14*, 2739–2753.

Andermann, T., Fernandes, A. M., Olsson, U., Töpel, M., Pfeil, B., Oxelman, B., … Antonelli, A. (2019). Allele phasing greatly improves the phylogenetic utility of ultraconserved elements. *Systematic Biology*, *68*, 32–46. https://doi.org/10.1093/sysbio/syy039

Bahr, A., Kaboth, S., Hodell, D., Zeeden, C., Fiebig, J., & Friedrich, O. (2018). Oceanic heat pulses fueling moisture transport towards continental Europe across the mid-Pleistocene transition. *Quaternary Science Reviews*, *179*, 48–58. https://doi.org/10.1016/j.quascirev.2017.11.009

Baker, H. G. (1967). Support for Baker's law – As a rule. *Evolution*, *21*, 853–856. https://doi.org/10.1111/j.1558-5646.1967.tb03440.x

Bierzychudek, P. (1985). Patterns in plant parthenogenesis. *Experientia*, *41*, 1255–1264. https://doi.org/10.1007/BF01952068

Bolger, A. M., Lohse, M., & Usade, B. (2014). Trimmomatic: A flexible trimmer for Illumina Sequence Data. *Bioinformatics*, *30*, 2114–2120. https://doi.org/10.1093/bioinformatics/btu170

Borowiec, M. L. (2016). AMAS: A fast tool for alignment manipulation and computing of summary statistics. *PeerJ*, *4*, e1660. https://doi.org/10.7717/peerj.1660

Bouckaert, R., Vaughan, T. G., Barido-Sottani, J., Duchêne, S., Fourment, M., Gavryushkina, A., … Drummond, A. J. (2019). BEAST 2.5: An advanced software platform for Bayesian evolutionary analysis. *PLoS Computational Biology*, *15*, e1006650.

Brewer, S., Cheddadi, R., de Beaulieu, J.-L., Reille, M., & Contributors, D. (2002). The spread of deciduous *Quercus* throughout Europe since the last glacial period. *Forest Ecology and Management*, *156*, 27–48. https://doi.org/10.1016/S0378-1127(01)00646-6

Capella-Gutiérrez, S., Silla-Martínez, J. M., & Gabaldón, T. (2009). trimAl: A tool for automated alignment trimming in large-scale phylogenetic analyses. *Bioinformatics*, *25*, 1972–1973. https://doi.org/10.1093/bioinformatics/btp348

Chamala, S., García, N., Godden, G. T., Krishnakumar, V., Jordon-Thaden, I. E., Smet, R. D., … Soltis, P. S. (2015). MarkerMiner 1.0: A new application for phylogenetic marker development using angiosperm transcriptomes. *Applications in Plant Sciences*, *3*, 1400115. https://doi.org/10.3732/apps.1400115

Chao, Z., Rabiee, M., Sayyari, E., & Mirarab, S. (2018). ASTRAL-III: Polynomial time species tree reconstruction from partially resolved gene trees. *BMC Bioinformatics*, *19*, 153. https://doi.org/10.1186/s12859-018-2129-y

Chen, L. Y., Zhao, S. Y., Wang, Q. F., & Moody, M. L. (2015). Transcriptome sequencing of three *Ranunculus* species (Ranunculaceae) reveals candidate genes in adaptation from terrestrial to aquatic habitats. *Scientific Reports*, *5*, e10098. https://doi.org/10.1038/srep10098

Clark, P. U., Archer, D., Pollard, D., Blum, J. D., Rial, J. A., Brovkin, V., … Roy, M. (2006). The middle Pleistocene transition: Characteristics, mechanisms, and implications for long-term changes in atmospheric pCO_2. *Quaternary Science Reviews*, *25*, 3150–3184. https://doi.org/10.1016/j.quascirev.2006.07.008

Comes, H. P., & Kadereit, J. W. (1998). The effect of Quaternary climatic changes on plant distribution and evolution. *Trends in Plant Science*, *3*, 432–438. https://doi.org/10.1016/S1360-1385(98)01327-2

R Core Team (2018). *R: A language and environment for statistical computing*. Vienna, Austria: R Foundation for Statistical Computing. Retrieved from http://www.r-project.org

Cosendai, A. C., Wagner, J., Ladinig, U., Rosche, C., & Hörandl, E. (2013). Geographical parthenogenesis and population genetic structure in the alpine species *Ranunculus kuepferi* (Ranunculaceae). *Heredity*, *110*, 560–569.

Couvreur, T. L. P., Pirie, M. D., Chatrou, L. W., Saunders, R. M. K., Su, Y. C. F., Richardson, J. E., & Erkens, R. H. J. (2011). Early evolutionary history of the flowering plant family Annonaceae: Steady diversification and boreotropical geodispersal. *Journal of Biogeography*, *38*, 664–680. https://doi.org/10.1111/j.1365-2699.2010.02434.x

Darriba, D., Taboada, G. L., Doallo, R., & Posada, D. (2012). jModelTest 2: More models, new heuristics and parallel computing. *Nature Methods*, *9*, 772. https://doi.org/10.1038/nmeth.2109

Després, L., Loriot, S., & Gaudeul, M. (2002). Geographic pattern of genetic variation in the European globeflower *Trollius europaeus* L. (Ranunculaceae) inferred from amplified fragment length polymorphism markers. *Molecular Ecology*, *11*, 2337–2347. https://doi.org/10.1046/j.1365-294X.2002.01618.x

Drummond, A. J., & Bouckaert, R. R. (2015). *Bayesian evolutionary analysis with BEAST*. Cambridge, UK: Cambridge University Press.

Dunkel, F. G. (2011). The *Ranunculus auricomus* L. complex (Ranunculaceae) in Central and Southern Italy, with additions to North Italian taxa. *Webbia*, *66*, 165–193.

Dunkel, F. G., Gregor, T., & Paule, J. (2018). New diploid species in the *Ranunculus auricomus* complex (Ranunculaceae) from W and SE Europe. *Willdenowia*, *48*, 227–257. https://doi.org/10.3372/wi.48.48205

Elderfield, H., Ferretti, P., Greaves, M., Crowhurst, S., McCave, I. N., Hodell, D., & Piotrowski, A. M. (2012). Evolution of ocean temperature and ice volume through the Mid-Pleistocene Climate Transition. *Science*, *337*, 704–709. https://doi.org/10.1126/science.1221294

Emadzade, K., Gehrke, B., Linder, H. P., & Hörandl, E. (2011). The biogeographical history of the cosmopolitan genus *Ranunculus* L. (Ranunculaceae) in the temperate to meridional zones. *Molecular Phylogenetics and Evolution*, *58*, 4–21. https://doi.org/10.1016/j.ympev.2010.11.002

Emadzade, K., & Hörandl, E. (2011). Northern Hemisphere origin, transoceanic dispersal, and diversification of Ranunculeae DC. (Ranunculaceae) in the Cenozoic. *Journal of Biogeography*, *38*, 517–530. https://doi.org/10.1111/j.1365-2699.2010.02404.x

Emadzade, K., Lebmann, M., Hoffmann, M. H., Tkach, N., Lone, F., & Hörandl, E. (2015). Phylogenetic relationships and evolution of high mountain buttercups (Ranunculus) in North America and Central Asia. *Perspectives in Plant Ecology, Evolution and Systematics*, *17*, 131–141. https://doi.org/10.1016/j.ppees.2015.02.001

Eriksson, J. S., de Sousa, F., Bertrand, Y. J. C., Antonelli, A., Oxelman, B., & Pfeil, B. E. (2018). Allele phasing is critical to revealing a shared allopolyploid origin of *Medicago arborea* and *M. strasseri* (Fabaceae). *BMC Evolutionary Biology*, *18*, 9. https://doi.org/10.1186/s12862-018-1127-z

Fér, T., & Schmickl, R. E. (2018). Hybphylomaker: Target enrichment data analysis from raw reads to species trees. *Evolutionary Bioinformatics*, *14*, 1–9. https://doi.org/10.1177/1176934317742613

Folk, R. A., Mandel, J. R., & Freudenstein, J. V. (2015). A protocol for targeted enrichment of intron-containing sequence markers for recent radiations: A phylogenomic example with genomic resources from *Heuchera* (Saxifragaceae). *Applications in Plant Sciences*, *3*, 1500039.

Fragoso-Martínez, I., Salazar, G. A., Martínez-Gordillo, M., Magallón, S., Sánchez-Reyes, L., Moriarty Lemmon, E., … Granados Mendoza, C. (2017). A pilot study applying the plant Anchored Hybrid Enrichment method to New World sages (*Salvia* subgenus *Calosphace*; Lamiaceae). *Molecular Phylogenetics and Evolution*, *117*, 124–134. https://doi.org/10.1016/j.ympev.2017.02.006

Gaboardi, M., Deng, T., & Wang, Y. (2005). Middle Pleistocene climate and habitat change at Zhoukoudian, China, from the carbon and oxygen isotopic record from herbivore tooth enamel. *Quaternary Research*, *63*, 329–338. https://doi.org/10.1016/j.yqres.2005.02.006

Giarla, T. C., & Esselstyn, J. (2015). The challenges of resolving a rapid, recent radiation: Empirical and simulated phylogenomics of Philippine shrews. *Systematic Biology*, *64*, 727–740. https://doi.org/10.1093/sysbio/syv029

Grummer, J. A., Morando, M. M., Avila, L. J., Sites, J. W. Jr, & Leaché, A. D. (2018). Phylogenomic evidence for a recent and rapid radiation of lizards in the Patagonian *Liolaemus ftzingerii* species group. *Molecular Phylogenetics and Evolution*, *125*, 243–254.

Harvey, M. G., Smith, B. T., Glenn, T. C., Faircloth, C. B., & Brumfield, R. T. (2016). Sequence capture versus restriction site associated DNA sequencing for shallow systematics. *Systematic Biology*, *65*, 910–924. https://doi.org/10.1093/sysbio/syw036

Head, M. J., & Gibbard, P. L. (2005). Early-Middle Pleistocene transitions: An overview and recommendation for the defining boundary. In M. L. Head, & E. L. Gibbard (Eds.), *Early-middle pleistocene transitions: The land-ocean evidence* (pp. 1–18). London, UK: Geological Society.

Herrando-Moraira, S., & The Cardueae Radiations Group (2018). Exploring data processing strategies in NGS target enrichment to disentangle radiations in the tribe Cardueae (Compositae). *Molecular Phylogenetics and Evolution*, *128*, 69–87. https://doi.org/10.1016/j.ympev.2018.07.012

Hewitt, G. M. (1999). Post-glacial re-colonization of European biota. *Biological Journal of the Linnean Society*, *68*, 87–112. https://doi.org/10.1111/j.1095-8312.1999.tb01160.x

Hojsgaard, D., Greilhuber, J., Pellino, M., Paun, O., Sharbel, T. F., & Hörandl, E. (2014). Emergence of apospory and bypass of meiosis via apomixis after sexual hybridisation and polyploidisation. *New Phytologist*, *204*, 1000–1012. https://doi.org/10.1111/nph.12954

Hörandl, E. (2004). Comparative analysis of genetic divergence among sexual ancestor of apomictic complexes using isozyme data. *International Journal of Plant Sciences*, *165*, 615–622.

Hörandl, E. (2006). The complex causality of geographical parthenogenesis. *New Phytologist*, *171*, 525–538. https://doi.org/10.1111/j.1469-8137.2006.01769.x

Hörandl, E. (2008). Evolutionary implications of self-compatibility and reproductive fitness in the apomictic *Ranunculus auricomus* polyploid complex (Ranunculaceae). *International Journal of Plant Sciences*, *169*, 1219–1228.

Hörandl, E., & Greilhuber, J. (2002). Diploid and autotetraploid sexuals and their relationships to apomicts in the *Ranunculus cassubicus* group: Insights from DNA content and isozyme variation. *Plant Systematics and Evolution*, *234*, 85–100.

Hörandl, E., Greilhuber, J., & Dobes, C. (2000). Isozyme variation and ploidy levels within the apomictic *Ranunculus auricomus* complex: Evidence for a sexual progenitor species in southeastern Austria. *Plant Biology*, *2*, 53–62. https://doi.org/10.1055/s-2000-9148

Hörandl, E., Greilhuber, J., Klímová, K., Paun, O., Temsch, E., Emadzade, K., & Hodálová, I. (2009). Reticulate evolution and taxonomic concepts in the *Ranunculus auricomus* complex (Ranunculaceae): Insights from analysis of morphological, karyological and molecular data. *Taxon*, *58*, 1194–1215.

Huson, D. H., & Bryant, D. (2006). Application of phylogenetic networks in evolutionary studies. *Molecular Biology and Evolution*, *23*, 254–267. https://doi.org/10.1093/molbev/msj030

Junier, T., & Zdobnov, E. M. (2010). The Newick utilities: High-throughput phylogenetic tree processing in the UNIX shell. *Bioinformatics*, *26*, 1669–1670. https://doi.org/10.1093/bioinformatics/btq243

Kadereit, J. W., Griebeler, E. M., & Comes, H. P. (2004). Quaternary diversification in European Alpine plants: Pattern and process. *Philosophical Transactions of the Royal Society B: Biological Sciences*, *359*, 265–274.

Karbstein, K., Tomasello, S., Hodač, L., Dunkel, F. G., Daubert, M., & Hörandl, E. (2020). Phylogenomics supported by geometric morphometrics reveals delimitation of sexual species within the polyploid apomictic *Ranunculus auricomus* complex (Ranunculaceae). *BioRxiv*. https://doi.org/10.1101/2020.01.07.896902

Katoh, K., & Standley, D. M. (2013). MAFFT multiple sequence alignment software version 7: Improvements in performance and usability. *Molecular Biology and Evolution*, *30*, 772–780. https://doi.org/10.1093/molbev/mst010

Kent, W. J. (2002). BLAT - The BLAST-like alignment tool. *Genome Research*, *12*, 656–664. https://doi.org/10.1101/gr.229202

Kirchheimer, B., Wessely, J., Gattringer, A., Hülber, K., Moser, D., Schinkel, C. C. F., … Dullinger, S. (2018). Reconstructing geographical parthenogenesis: Effects of niche differentiation and reproductive mode on Holocene range expansion of an alpine plant. *Ecology Letters*, *21*, 392–401. https://doi.org/10.1111/ele.12908

Knapp, M., Stöckler, K., Havell, D., Delsuc, F., Sebastiani, F., & Lockhart, P. (2005). Relaxed molecular clock provides evidence for long-distance dispersal of *Nothofagus* (southern beech). *PLoS Biology*, *3*, e14. https://doi.org/10.1371/journal.pbio.0030014

Knowles, L. L. (2001). Did the Pleistocene glaciations promote divergence? Tests of explicit refugial models in montane grasshoppers. *Molecular Ecology*, *10*, 691–701.

Knowles, L. L., & Chan, Y.-H. (2008). Resolving species phylogenies of recent evolutionary radiations. *Annals of the Missouri Botanical Garden*, *95*, 224–231.

Kramp, K., Huck, S., Niketić, M., Tomović, G., & Schmitt, T. (2008). Multiple glacial refugia and complex postglacial range shifts of the obligatory woodland plant *Polygonatum verticillatum* (Convallariaceae). *Plant Biology*, *11*, 392–404.

Kropf, M., Kadereit, J. W., & Comes, H. P. (2003). Differential cycles of range contraction and expansion in European high mountain plants during the Late Quaternary: Insights from *Pritzelago alpina* (L.) O. Kuntze (Brassicaceae). *Molecular Ecology*, *12*, 931–949. https://doi.org/10.1046/j.1365-294X.2003.01781.x

Kubatko, L. S., & Degnan, J. H. (2007). Inconsistency of phylogenetic estimates from concatenated data under coalescence. *Systematic Biology*, *56*, 17–24. https://doi.org/10.1080/10635150601146041

Kumar, S., Filipski, A. J., Battistuzzi, F. U., Pond, S. L. K., & Tamura, K. (2012). Statistics and truth in phylogenomics. *Molecular Biology and Evolution*, *29*, 457–472. https://doi.org/10.1093/molbev/msr202

Levin, D. (1975). Minority cytotype exclusion in local plant populations. *Taxon*, *24*, 35–43. https://doi.org/10.2307/1218997

Li, H., Handsaker, B., Wysoker, A., Fennell, T., Ruan, J., & Homer, N., …1000 Genome Project Data Processing Subgroup (2009). The sequence alignment/map format and SAMtools. *Bioinformatics*, *25*, 2078–2079. https://doi.org/10.1093/bioinformatics/btp352

Li, H., & Durbin, R. (2009). Fast and accurate short read alignment with Burrows-Wheeler transform. *Bioinformatics*, *25*, 1754–1760. https://doi.org/10.1093/bioinformatics/btp324

Lisiecki, L. L., & Raymo, M. E. (2005). A Pliocene-Pleistocene stack of 57 globally distributed benthic $\delta^{18}O$ records. *Paleoceanography*, *20*, PA1003. https://doi.org/10.1029/2004PA001071

López-Giráldez, F., & Townsend, J. P. (2011). PhyDesign: An online application for profiling phylogenetic informativeness. *BMC Evolutionary Biology*, *11*, 152. https://doi.org/10.1186/1471-2148-11-152

Magri, D. (2008). Patterns of post-glacial spread and the extent of glacial refugia of European beech (*Fagus sylvatica*). *Journal of Biogeography*, *35*, 450–463. https://doi.org/10.1111/j.1365-2699.2007.01803.x

Magri, D., & Palombo, M. R. (2013). Early to Middle Pleistocene dynamics of plant and mammal communities in South West Europe. *Quaternary International*, *288*, 63–72. https://doi.org/10.1016/j.quaint.2012.02.028

Magri, D., Vendramin, G. G., Comps, B., Dupanloup, I., Geburek, T., Gomory, D., … de Beaulieu, J.-L. (2006). A new scenario for the Quaternary history of European beech populations: Palaeobotanical evidence and genetic consequences. *New Phytologist*, *171*, 199–221. https://doi.org/10.1111/j.1469-8137.2006.01740.x

Masci, S., Miho, A., & Marchi, P. (1994). *Ranunculus auricomus* L. aggr. (Ranunculaceae) in Italy. I. Sexual tetraploids on the Apennines . *Caryologia*, *47*, 97–108.

Matzke, N. J. (2013). Probabilistic historical biogeography:New models for founder-event speciation, imperfect detection, and fossils allow improved accuracy and model-testing. *Frontiers of Biogeography*, *5*, 242–248. https://doi.org/10.21425/F55419694

Matzke, N. J. (2018). *BioGeoBEARS: BioGeography with Bayesian (and likelihood) evolutionary analysis with R scripts*. *Version 1.1.1*. Retrieved from https://doi.org/10.5281/zenodo.1478250

McCormack, J. E., Harvey, M. G., Faircloth, B. C., Crawford, N. G., Glenn, T. C., & Brumfield, R. T. (2013). A phylogeny of birds based on over 1,500 loci collected by target enrichment and high-throughput sequencing. *PLoS ONE*, *8*, e54848. https://doi.org/10.1371/journal.pone.0054848

McKain, M. R., Johnson, M. G., Uribe-Convers, S., Eaton, D., & Yang, Y. (2018). Practical considerations for plant phylogenomics. *Applications in Plant Sciences*, *6*, e1038. https://doi.org/10.1002/aps3.1038

Naydenov, K., Senneville, S., Beaulieu, J., Tremblay, F., & Bousquet, J. (2007). Glacial vicariance in Eurasia: Mitochondrial DNA evidence from Scots pine for a complex heritage involving genetically distinct refugia at mid-northern latitudes and in Asia Minor. *BMC Evolutionary Biology*, *7*, 233. https://doi.org/10.1186/1471-2148-7-233

Nei, M. (1975). Molecular population genetics and evolution. *Frontiers in Biology*, *40*, 1–288.

Paradis, E., & Schliep, K. (2018). ape 5.0: An environment for modern phylogenetics and evolutionary analyses in R. *Bioinformatics*, *35*, 526–528. https://doi.org/10.1093/bioinformatics/bty633

Pastre, J.-F., Gauthier, A., Nomade, S., Orth, P., Andrieu, A., Goupille, F., … Renne, P. R. (2007). The Alleret maar (Massif Central, France): A new lacustrine sequence of the early Middle Pleistocene in western Europe. *Comptes Rendus Geoscience*, *339*, 987–997. https://doi.org/10.1016/j.crte.2007.09.019

Paun, O., Stuessy, T. F., & Hörandl, E. (2006). The role of hybridization, polyploidization and glaciation in the origin and evolution of the apomictic *Ranunculus cassubicus* complex. *New Phytologist*, *171*, 223–236. https://doi.org/10.1111/j.1469-8137.2006.01738.x

Pease, J. B., Brown, J. W., Walker, J. F., Hinchliff, C. E., & Smith, S. A. (2018). Quartet Sampling distinguishes lack of support from conflicting support in the green plant tree of life. *American Journal of Botany*, *105*, 385–403. https://doi.org/10.1002/ajb2.1016

Pellino, M., Hojsgaard, D., Schmutzer, T., Scholz, U., Hörandl, E., Vogel, H., & Sharbel, T. F. (2013). Asexual genome evolution in the apomictic *Ranunculus auricomus* complex: Examining the effects of hybridization and mutation accumulation. *Molecular Ecology*, *22*, 5908–5921.

Pond, S. L. K., Frost, S. D. W., & Muse, S. V. (2005). HyPhy: Hypothesis testing using phylogenies. *Bioinformatics*, *21*, 676–679. https://doi.org/10.1093/bioinformatics/bti079

Price, M. N., Dehal, P. S., & Arkin, A. P. (2010). FastTree 2 – Approximately maximum-likelihood trees for large alignments. *PLoS ONE*, *5*, e9490. https://doi.org/10.1371/journal.pone.0009490

Qiu, Y.-X., Guan, B.-C., Fu, C.-X., & Comes, H. P. (2009). Did glacials and/or interglacials promote allopatric incipient speciation in East Asian temperate plants? Phylogeographic and coalescent analyses on refugial isolation and divergence in *Dysosma versipellis*. *Molecular Phylogenetics and Evolution*, *51*, 281–293. https://doi.org/10.1016/j.ympev.2009.01.016

Rambaut, A., & Drummond, A. J. (2007). *Tracer v1.4: MCMC trace analyses tool*. Retrieved from http://beast.bio.ed.ac.uk/Tracer

Raymo, M. E., Lisiecki, L. E., & Nisancioglu, K. H. (2006). Plio-Pleistocene ice volume, antarctic climate, and the global $\delta^{18}O$ record. *Science*, *313*, 492–495.

Reisch, C. (2008). Glacial history of *Saxifraga paniculata* (Saxifragaceae): Molecular biogeography of a disjunct arcticalpine species from Europe and North America. *Biological Journal of the Linnean Society*, *93*, 385–398. https://doi.org/10.1111/j.1095-8312.2007.00933.x

Ronquist, F., & Sanmartín, I. (2011). Phylogenetic methods in biogeography. *Annual Review of Ecology, Evolution, and Systematics*, *42*, 441–464. https://doi.org/10.1146/annurev-ecolsys-102209-144710

Rull, V. (2009). Microrefugia. *Journal of Biogeography*, *36*, 481–484. https://doi.org/10.1111/j.1365-2699.2008.02023.x

Sánchez Goñi, M. F., Rodrigues, T., Hodell, D. A., Polanco-Martínez, J. M., Alonso-García, M., Hernández-Almeida, I., … Ferretti, P. (2016). Tropically-driven climate shifts in southwestern Europe during MIS 19, a low eccentricity interglacial. *Earth and Planetary Science Letters*, *448*, 81–93. https://doi.org/10.1016/j.epsl.2016.05.018

Sanderson, M. J. (2002). Estimating absolute rates of molecular evolution and divergence times: A penalized likelihood approach. *Molecular Biology Evolution*, *19*, 101–109. https://doi.org/10.1093/oxfordjournals.molbev.a003974

Sanmartín, I. (2009). Dispersal versus vicariance. In McGraw-Hill (Ed.), *Yearbook of Science and Technology* (pp. 85–88). New York, NY: McGraw-Hill.

Sanmartín, I. (2012). Historical biogeography: Evolution in time and space. *Evolution: Education and Outreach*, *5*, 555–568. https://doi.org/10.1007/s12052-012-0421-2

Sanz, M., Schönswetter, P., Vallés, J., Schneeweiss, G. M., & Vilartesana, R. (2014). Southern isolation and northern long distance dispersal shaped the phylogeography of the widespread, but highly disjunct, European high mountain plant *Artemisia eriantha* (Asteraceae). *Botanical Journal of the Linnean Society*, *174*, 214–226.

Sayyari, E., & Mirarab, S. (2016). Fast coalescent-based computation of local branch support from quartet frequencies. *Molecular Biology and Evolution*, *33*, 1654–1668. https://doi.org/10.1093/molbev/msw079

Schönswetter, P., Stehlik, I., Holderegger, R., & Tribsch, A. (2005). Molecular evidence for glacial refugia of mountain plants in the European Alps. *Molecular Ecology*, *14*, 3547–3555. https://doi.org/10.1111/j.1365-294X.2005.02683.x

Schönswetter, P., & Tribsch, A. (2005). Vicariance and dispersal in the Alpine perennial, *Bupleurum stellatum* L. (Apiaceae). *Taxon*, *54*, 725–732.

Stamatakis, A. (2014). RAxML version 8: A tool for phylogenetic analysis and post-analysis of large phylogenies. *Bioinformatics*, *30*, 1312–1313. https://doi.org/10.1093/bioinformatics/btu033

Stebbins, G. L. (1984). Polyploidy and the distribution of the Arctic-Alpine flora: New evidence and a new approach. *Botanica Helvetica*, *94*, 1–13.

Stephens, J. D., Rogers, W. L., Heyduk, K., Cruse-Sanders, J. M., Determann, R. O., Glenn, T. C., & Malmberg, R. L. (2015). Resolving phylogenetic relationships for the recently radiated carnivorous plant genus *Sarracenia* using target enrichment. *Molecular Phylogenetics and Evolution*, *85*, 76–87.

Stuchlik, L., & Wójcik, A. (2001). Pollen analysis of Malopolanian Interglacial deposits at Lowisko (Kolbuszowa Upland, southern Poland). *Acta Palaeobotanica*, *41*, 15–26.

Taberlet, P., Fumagalli, L., Wust-Saucy, A. G., & Cosson, J.-F. (1998). Comparative phylogeography and postglacial colonization routes in Europe. *Molecular Ecology*, *7*, 453–464. https://doi.org/10.1046/j.1365-294x.1998.00289.x

Tomasello, S., & Oberprieler, C. (2017). Frozen ploidies: A phylogeographical analysis of the *Leucanthemopsis alpina* polyploid complex (Asteraceae, Anthemideae). *Botanical Journal of the Linnean Society*, *183*, 211–235. https://doi.org/10.1093/botlinnean/bow009

Townsend, J. P. (2007). Profiling phylogenetic informativeness. *Systematic Biology*, *56*, 222–231. https://doi.org/10.1080/10635150701311362

Tribsch, A., Schönswetter, P., & Stuessy, T. F. (2002). *Saponaria pumila* (Caryophyllaceae) and the ice age in the European Alps. *American Journal of Botany*, *89*, 2024–2033. https://doi.org/10.3732/ajb.89.12.2024

Van Dam, M., & Matzke, N. J. (2016). Evaluating the influence of connectivity and distance on biogeographic patterns in the south-western deserts of North America. *Journal of Biogeography*, *43*, 1514–1532.

Vargas, P. (2003). Molecular evidence for multiple diversification patterns of Alpine plants in Mediterranean Europe. *Taxon*, *52*, 463–476. https://doi.org/10.2307/3647383

Weisrock, D. W., Smith, S. D., Chan, L. M., Biebouw, K., Kappeler, P. M., & Yoder, A. D. (2012). Concatenation and concordance in the reconstruction of mouse lemur phylogeny: An empirical demonstration of the effect of allele sampling in phylogenetics. *Molecular Biology and Evolution*, *29*, 1615–1630. https://doi.org/10.1093/molbev/mss008

Weitemier, K., Straub, S. C., Cronn, R. C., Fishbein, M., Schmickl, R., McDonnell, A., & Liston, A. (2014). Hyb-Seq: Combining target enrichment and genome skimming for plant phylogenomics. *Applications in Plant Sciences*, *2*, 1400042. https://doi.org/10.3732/apps.1400042

Widmer, A., & Lexer, C. (2001). Glacial refugia: Sanctuaries for allelic richness, but not for gene diversity. *Trends in Ecology and Evolution*, *16*, 267–269. https://doi.org/10.1016/S0169-5347(01)02163-2

Wolfe, K. H., Gouy, M. L., Yang, Y. W., Sharp, P. M., & Li, W. H. (1989). Date of the monocot dicot divergence estimated from chloroplast dna-sequence data. *Proceedings of the National Academy of Sciences of the United States of America*, *86*, 6201–6205. https://doi.org/10.1073/pnas.86.16.6201

Xu, H., Luo, X., Qian, J., Pang, X., Song, J., Qian, G., … Chen, S. (2012). FastUniq: A fast de novo duplicates removal tool for paired short reads. *PLoS ONE*, *7*, e52249. https://doi.org/10.1371/journal.pone.0052249

Yang, Z. (2007). PAML 4: Phylogenetic analysis by maximum likelihood. *Molecular Biology and Evolution*, *24*, 1586–1591. https://doi.org/10.1093/molbev/msm088

Zhao, C., Wang, C. B., Ma, X. G., Liang, Q. L., & He, X. J. (2013). Phylogeographic analysis of a temperate-deciduous forest restricted plant (*Bupleurum longiradiatum* Turcz.) reveals two refuge areas in China with subsequent refugial isolation promoting speciation. *Molecular Phylogenetics and Evolution*, *68*, 628–643. https://doi.org/10.1016/j.ympev.2013.04.007

Zhao, W., Tarasov, P. E., Lozhkin, A. V., Anderson, P. M., Andreev, A. A., Korzun, J. A., … Wennrich, V. (2017). High-latitude vegetation and climate changes during the Mid-Pleistocene Transition inferredfrom apalynological record from Lake El'gygytgyn, NE Russian Arctic. *Boreas*, *47*, 137–149. https://doi.org/10.1111/bor.12262

Zhou, X., Yang, J., Wang, S., Xiao, G., Zhao, K., Zheng, Y., … Li, X. (2018). Vegetation change and evolutionary response of large mammal fauna during the Mid-Pleistocene Transition in temperate northern East Asia. *Palaeogeography Palaeoclimatology Palaeoecology*, *505*, 287–292. https://doi.org/10.1016/j.palaeo.2018.06.007

SUPPORTING INFORMATION

Additional supporting information may be found online in the Supporting Information section.

How to cite this article: Tomasello S, Karbstein K, Hodač L, Paetzold C, Hörandl E. Phylogenomics unravels Quaternary vicariance and allopatric speciation patterns in temperate-montane plant species: A case study on the *Ranunculus auricomus* species complex. *Mol Ecol*. 2020;00:1–19. https://doi.org/10.1111/mec.15458